

GRADIENT-ADJUSTED UNDERDAMPED LANGEVIN DYNAMICS FOR SAMPLING*

XINZHE ZUO[†], STANLEY OSHER[†], AND WUCHEN LI[‡]

Abstract. Sampling from a target distribution is a fundamental problem with wide-ranging applications in scientific computing and machine learning. Traditional Markov chain Monte Carlo (MCMC) algorithms, such as the unadjusted Langevin algorithm (ULA), derived from the overdamped Langevin dynamics, have been extensively studied. From an optimization perspective, the Kolmogorov forward equation of the overdamped Langevin dynamics can be treated as the gradient flow of the relative entropy in the space of probability densities embedded with Wasserstein-2 metrics. Several efforts have also been devoted to including momentum-based methods, such as underdamped Langevin dynamics for faster convergence of sampling algorithms. Recent advances in optimizations have demonstrated the effectiveness of primal-dual damping and Hessian-driven damping dynamics for achieving faster convergence in solving optimization problems. Motivated by these developments, we introduce a class of stochastic differential equations (SDEs) called gradient-adjusted underdamped Langevin dynamics (GAUL), which add stochastic perturbations in primal-dual damping dynamics and Hessian-driven damping dynamics from optimization. We prove that GAUL admits the correct stationary distribution, whose marginal is the target distribution. The proposed method outperforms overdamped and underdamped Langevin dynamics regarding convergence speed in the total variation distance for Gaussian target distributions. Moreover, using the Euler-Maruyama discretization, we show that the mixing time towards a biased target distribution only depends on the square root of the condition number of the target covariance matrix. Numerical experiments for non-Gaussian target distributions, such as Bayesian regression problems and Bayesian neural networks, further illustrate the advantages of our approach over classical methods based on overdamped or underdamped Langevin dynamics.

Key words. Hessian-driven damping dynamics; Primal-dual damping dynamics; Nesterov’s method; Langevin dynamics; Optimal convergence rate.

MSC codes. 37M25, 65C05, 82C31.

1. Introduction. Sampling from a target distribution is a long-standing quest and has numerous applications in scientific computing, including Bayesian statistical inference [46, 53, 43, 31], Bayesian inverse problems [56, 35, 23, 29], as well as Bayesian neural networks [65, 2, 61, 36, 45, 51]. In this direction, various algorithms have been developed to sample a target distribution $\pi \propto \exp(-f)$ for a given function $f : \mathbb{R}^d \rightarrow \mathbb{R}$, where π is only known up to a normalization constant. In this area, a simple and popular algorithm is the unadjusted Langevin algorithm (ULA):

$$(1.1) \quad \mathbf{x}_{k+1} = \mathbf{x}_k - h\nabla f(\mathbf{x}_k) + \sqrt{2h}\mathbf{z}_k,$$

where $\mathbf{x}_k \in \mathbb{R}^d$, k is the iteration number, f is assumed to be a differentiable function, $h > 0$ is a step size, and \mathbf{z}_k is a d -dimensional random variable with independently and identically distributed (i.i.d) entries following standard Gaussian distributions. The ULA algorithm (1.1) comes from the forward Euler discretization of a stochastic differential equation (SDE) known as overdamped Langevin dynamics:

$$(1.2) \quad d\mathbf{x}_t = -\nabla f(\mathbf{x}_t)dt + \sqrt{2}d\mathbf{B}_t,$$

*Submitted to the editors DATE.

[†]Department of Mathematics, University of California, Los Angeles, CA, 90095. ({zxx,sjo}@math.ucla.edu).

[‡]Department of Mathematics, University of South Carolina, Columbia, SC, 29208. (wuchen@mailbox.sc.edu).

42 where $\mathbf{x}_t \in \mathbb{R}^d$ and \mathbf{B}_t is a standard d -dimensional Brownian motion. Under some
 43 mild conditions on f , it has been shown that the SDE (2.15) has a unique strong
 44 solution $\{\mathbf{x}_t, t \geq 0\}$ that is a Markov process [54, 49]. Moreover, the distribution of
 45 \mathbf{x}_t converges to the invariant distribution $\pi \propto \exp(-f)$ as $t \rightarrow \infty$. The asymptotic
 46 convergence guarantees of (1.1) have been established decades ago [59, 30, 48]. In
 47 more recent years, non-asymptotic behaviors of (1.1) have also been explored by
 48 several works [19, 20, 26, 21, 15, 63].

49 An important result by [37] states that the Kolmogorov forward equation of
 50 Langevin dynamics corresponds to the gradient flow of the relative entropy func-
 51 tional in the space of probability density functions with the Wasserstein-2 metric.
 52 This observation serves as a bridge between the sampling community and the opti-
 53 mization community by studying optimization problems in Wasserstein-2 space. In
 54 the field of optimization, Nesterov’s accelerated gradient [52] is a first order algorithm
 55 for finding the minimum of a convex/strongly convex objective function f . The in-
 56 tuition is that Nesterov’s method incorporates momentum into the updates. It is
 57 much faster than the traditional gradient descent method, in the sense that the con-
 58 vergence speed for convex functions is $\mathcal{O}(\frac{1}{k^2})$ where k is the number of iterations
 59 compared to $\mathcal{O}(\frac{1}{k})$ for gradient descent. The convergence speed of Nesterov’s method
 60 for L -smooth, m -strongly convex functions is $\mathcal{O}(\exp(-k/\sqrt{\kappa}))$ where $\kappa = L/m$ is the
 61 condition number of f compared to $\mathcal{O}(\exp(-k/\kappa))$ for gradient descent. By taking
 62 the step size to 0, one obtains a second-order ODE for Nesterov’s method called the
 63 Nesterov’s accelerated gradient flow or Nesterov’s ODE [57, 5]. In recent years, one
 64 extends the gradient flow of the relative entropy into Nesterov’s accelerated gradient
 65 flow [57], which is explored in [64, 58, 44] from different perspectives. For the opti-
 66 mization in Wasserstein-2 space perspective, [64, 58, 13] study a class of accelerated
 67 dynamics with depending on the score function, i.e., the gradient of logarithm of den-
 68 sity function. This results in the approximation of a non-linear partial differential
 69 equation, known as the damped Euler equation [10]. In this case, the optimal choices
 70 of parameters for sampling a target distribution share similarities with the classical
 71 Nesterov’s accelerated gradient flow. On the other hand, from a stochastic dynamics
 72 perspective, a line of research has been devoted to study the accelerated version of
 73 Langevin dynamics, known as the underdamped Langevin dynamics [9, 16, 44, 66].
 74 As explained later in Subsection 2.2, the underdamped Langevin dynamics consists
 75 of a deterministic component and a stochastic component. The deterministic compo-
 76 nent exactly corresponds to the Nesterov’s accelerated gradient flow. The marginal of
 77 invariant distribution in x -axis satisfies the target distribution. However, the optimal
 78 choice of parameters in underdamped Langevin dynamics might not directly follow
 79 the classical Nesterov’s method [16].

Recently, [67] proposed to use the primal-dual hybrid gradient (PDHG) method
 [12, 62] to solve unconstrained optimization problems. The original PDHG method
 is designed for optimization problem with linear constraints. [67] formulated the
 optimality condition $\nabla f(\mathbf{x}) = 0$ of a strongly convex function f into the solution of a
 saddle point problem

$$\inf_{\mathbf{x} \in \mathbb{R}^d} \sup_{\mathbf{p} \in \mathbb{R}^d} \langle \nabla f(\mathbf{x}), \mathbf{p} \rangle - \frac{\gamma}{2} \|\mathbf{p}\|^2,$$

80 where $\gamma > 0$ is a selected regularization parameter. They proceed by using the
 81 PDHG algorithm with appropriate preconditioners to solve the above saddle point
 82 problem. By taking the limit as the step size goes to zero, their algorithm yields a
 83 continuous-time flow, which is a second-order ordinary differential equation (ODE)

84 called the primal-dual damping (PDD) dynamics. In particular, the PDD dynamic
 85 contains Nesterov’s ODE [57]. In other words, Nesterov’s ODE is a special case
 86 of PDD dynamics. The PDD dynamics also shares similarities with the Hessian–
 87 driven damping dynamics that has been studied in recent years [5, 3, 4]. The main
 88 difference between the PDD dynamics and the Nesterov’s ODE is a second-order term
 89 $\nabla^2 f(\mathbf{x})\dot{\mathbf{x}}$ that appears in the former. This term is also presented in the Hessian driven
 90 damping dynamics. It has been observed that the PDD dynamics and the Hessian
 91 driven damping dynamics yield faster convergence towards the global minimum than
 92 the traditional gradient flow and Nesterov’s ODE. Therefore, it is natural to extend
 93 the PDD dynamics and Hessian driven damping dynamics to SDEs for sampling a
 94 target distribution.

95 In this paper, we take inspirations from [67, 3] to design a system of SDE
 96 called gradient-adjusted underdamped Langevin dynamics (GAUL) that resembles
 97 the primal-dual damping dynamics and the Hessian driven damping dynamics. Con-
 98 sider

$$99 \quad (1.3) \quad \begin{pmatrix} d\mathbf{x}_t \\ d\mathbf{p}_t \end{pmatrix} = \begin{pmatrix} -a\mathbf{C}\nabla f(\mathbf{x}_t)dt + \mathbf{C}\mathbf{p}_t dt \\ -\nabla f(\mathbf{x}_t)dt - \gamma\mathbf{p}_t dt \end{pmatrix} + \sqrt{\begin{pmatrix} 2a\mathbf{C} & \mathbf{I} - \mathbf{C} \\ \mathbf{I} - \mathbf{C} & 2\gamma\mathbf{I} \end{pmatrix}} \begin{pmatrix} d\mathbf{B}_t^{(1)} \\ d\mathbf{B}_t^{(2)} \end{pmatrix},$$

100 for some constants $a, \gamma > 0$, whose detailed choices will be explained later. \mathbf{C} is a
 101 preconditioner such that the diffusion matrix in front of the Brownian motion term is
 102 well-defined and positive semidefinite. And $\mathbf{B}_t^{(i)}$ is a standard Brownian motion in \mathbb{R}^d
 103 for $i = 1, 2$. The superscript on \mathbf{B}_t indicates that $\mathbf{B}_t^{(1)}$ and $\mathbf{B}_t^{(2)}$ are independent. We
 104 show that the stationary distribution GAUL (1.3) is the desired target distribution
 105 of the form $\frac{1}{Z} \exp(-f(\mathbf{x}) - \|\mathbf{p}\|^2/2)$. Noticeably, the \mathbf{x} -marginal distribution is the
 106 target distribution π . Additionally, we demonstrate that for a quadratic function f ,
 107 GAUL achieves the exponential convergence and outperforms both overdamped and
 108 underdamped Langevin dynamics. A series of numerical examples are provided to
 109 demonstrate the advantage of the proposed method.

110 To illustrate the main idea, we summarize main theoretical results into the fol-
 111 lowing informal theorem.

112 **THEOREM 1.1 (Informal).** *Suppose that $f : \mathbb{R}^d \rightarrow \mathbb{R}^d$ is given by $f(\mathbf{x}) = \frac{1}{2}\mathbf{x}^T \Lambda \mathbf{x}$*
 113 *with a symmetric positive definite matrix $\Lambda \in \mathbb{R}^{d \times d}$ with eigenvalues $s_1 \geq s_2 \geq \dots \geq$*
 114 *$s_d > 0$. Let $\kappa = s_1/s_d$ be the condition number of matrix Λ . And let $\mathbf{C} = \mathbf{I}$.*

- 115 (1) *Denote by $\rho_x(\mathbf{x}, t)$ the law of \mathbf{x}_t driven by (1.3), and $\pi(\mathbf{x}) \propto \exp(-f(\mathbf{x}))$*
 116 *the target distribution. Let $a > 0$, $\gamma = as_d + 2\sqrt{s_d}$. Then it takes at most*
 117 *$t = \mathcal{O}(\log(d/\delta))/(as_d + 2\sqrt{s_d})$ for the total variation distance between $\rho_x(\mathbf{x}, t)$*
 118 *and $\pi(\mathbf{x})$ to decrease to δ .*
- 119 (2) *Denote by $\tilde{\rho}_x(\mathbf{x}, k)$ the law of \mathbf{x} after k iterations of the Euler-Maruyama*
 120 *discretization of (1.3). Suppose $\sqrt{s_1} - \sqrt{s_d} \geq 2$, $a = 1$, $\gamma = s_d + 2\sqrt{s_d}$ and*
 121 *consider the Euler-Maruyama discretization of (1.3) with step size $h = 1/5s_1$.*
 122 *Then it takes at most $N = \mathcal{O}(\log(d/\delta)/(\kappa^{-1} + (\kappa s_1)^{-1/2}))$ iterations for the*
 123 *total variation distance between $\tilde{\rho}_x(\mathbf{x}, k)$ and $\tilde{\pi}(\mathbf{x})$ to decrease to δ , where*
 124 *$\tilde{\pi}(\mathbf{x})$ is a biased target distribution given by Equation (B.24).*
- 125 (3) *When taking $a = \frac{2}{\sqrt{s_1} - \sqrt{s_d}}$, $\gamma = as_d + 2\sqrt{s_d}$ and $h = \frac{1}{2(as_1 + \gamma)}$, we can improve*
 126 *the number of iterations in (2) to $N = \mathcal{O}(\sqrt{\kappa} \log(d/\delta))$.*

127 The detailed version of Theorem 1.1 is given in Theorem 3.9, Theorem 3.15 and The-
 128 orem 3.16. It is worth noting that GAUL (1.3) reduces to underdamped Langevin
 129 dynamics when $a = 0$ and $\mathbf{C} = \mathbf{I}$. Our theorem implies that in the Gaussian case,

GAUL converges to the target measure faster than underdamped Langevin dynamics. In particular, we demonstrate that the Euler-Maruyama discretization admits a mixing time proportional to the square root of the condition number of covariance matrix. While this work primarily focuses on Gaussian distributions, our numerical experiments also explore non-log-concave target distributions in Bayesian linear regressions and Bayesian neural networks, which demonstrate potential advantages of GAUL over overdamped and underdamped Langevin dynamics. Extending these results to more general distributions and discretization schemes is an important future research direction. The choice of preconditioner \mathbf{C} is tricky as one needs to guarantee that the diffusion matrix in (1.3) is positive semidefinite. Therefore, we mainly focus on the case when $\mathbf{C} = \mathbf{I}$. We address our results for $\mathbf{C} \neq \mathbf{I}$ in Remark 3.10 and Remark 3.19. For $\mathbf{C} = \mathbf{I}$, [42] also explored dynamics (1.3), which they called Hessian-Free High-Resolution (HFHR) dynamics. For this closely related work, we provide some comparisons later in Remark 2.4.

This paper is organized as follows. In Section 2, we review the connection between optimization methods and sampling dynamics, which leads to the construction of our proposed SDE called gradient-adjusted underdamped Langevin dynamics (GAUL). Our main results are presented in Section 3, where we prove the exponential convergence of GAUL to the target distribution when the target measure follows a Gaussian distribution. We also study the Euler-Maruyama discretization of GAUL and prove its linear convergence to a biased target distribution. Lastly, in Section 4, we present several numerical examples to compare GAUL with both overdamped and underdamped Langevin dynamics.

2. Preliminaries. In this section, we briefly review the relation among Euclidean gradient flows, overdamped Langevin dynamics and Wasserstein gradient flows. We then draw the connection between the underdamped Langevin dynamics and Nesterov's ODEs. We next review primal-dual damping (PDD) flows [67] and Hessian driven damping dynamics. Finally, we introduce a new SDE called gradient-adjusted underdamped Langevin dynamics (GAUL) for sampling, which resembles the PDD flow and the Hessian-driven damping dynamics with designed stochastic perturbations in terms of Brownian motions.

2.1. Gradient descent, unadjusted Langevin algorithms, and optimal transport gradient flows. Let $f : \mathbb{R}^d \rightarrow \mathbb{R}$ be a differentiable convex function with L -Lipschitz gradient. The classical gradient descent algorithm for finding the global minimum of $f(\mathbf{x})$ is an iterative algorithm that reads:

$$(2.1) \quad \mathbf{x}_{k+1} = \mathbf{x}_k - h\nabla f(\mathbf{x}_k),$$

where $h > 0$ is the step size. When f is convex and the step size is not too large, this algorithm converges at a rate of $\mathcal{O}(k^{-1})$. When f is m -strongly convex, the same algorithm can be shown to converge at a rate of $\mathcal{O}((1 - m/L)^k)$, if the step size is chosen appropriately. The gradient descent algorithm (2.1) can be understood as the forward Euler time discretization of the gradient flow

$$(2.2) \quad \dot{\mathbf{x}}(t) = -\nabla f(\mathbf{x}(t)),$$

where $\mathbf{x}(t)$ describes a trajectory in \mathbb{R}^d that travels in the direction of the steepest descent. Similar convergence results can be obtained for the gradient flow (2.2). When f is convex, the gradient flow (2.2) converges at a rate of $\mathcal{O}(t^{-1})$. When f is assumed to be m -strongly convex, the gradient flow (2.2) converges at a rate of $\mathcal{O}(\exp(-mt))$.

While the goal of optimization is to find the global minimum of f , the goal of sampling algorithm is to sample from a distribution of the form $\frac{1}{Z_1} \exp(-f(\mathbf{x}))$, where the normalization constant $Z_1 > 0$ is assumed to be finite, i.e.,

$$Z_1 = \int_{\mathbb{R}^d} e^{-f(\mathbf{x})} d\mathbf{x} < +\infty.$$

The classical unadjusted Langevin algorithm (ULA) given in (1.1) is a simple modification to the gradient descent method. Recall that ULA is given by

$$(2.3) \quad \mathbf{x}_{k+1} = \mathbf{x}_k - h\nabla f(\mathbf{x}_k) + \sqrt{2h}\mathbf{z}_k,$$

where \mathbf{z}_k is a d -dimensional standard Gaussian random variable and h is the step size. We obtain (2.3) from (2.1) by adding a Gaussian noise term \mathbf{z}_k scaled by $\sqrt{2h}$. Similar to how (2.1) can be viewed as the Euler discretization of (2.2), ULA (2.3) represents the forward Euler discretization of the overdamped Langevin dynamics:

$$(2.4) \quad d\mathbf{x}_t = -\nabla f(\mathbf{x}_t)dt + \sqrt{2d}\mathbf{B}_t,$$

where \mathbf{B}_t is a standard d -dimensional Brownian motion. Denote by $\rho(\mathbf{x}, t)$ the probability density function for \mathbf{x}_t . Then the Kolmogorov forward equation (also known as the Fokker-Planck equation) of the overdamped Langevin dynamics (2.4) is given as

$$(2.5) \quad \frac{\partial \rho}{\partial t} = \nabla \cdot (\rho \nabla f) + \Delta \rho.$$

Clearly, $\pi(\mathbf{x}) = \frac{1}{Z_1} \exp(-f(\mathbf{x}))$ is a stationary solution of the Fokker-Planck equation (2.5). In other words, note that $\nabla \pi = -\pi \nabla f$, then

$$0 = \partial_t \pi = \nabla \cdot (\pi \nabla f) + \Delta \pi = \nabla \cdot ((\pi \nabla f) + \nabla \pi).$$

In the literature, one can also study the gradient drift Fokker-Planck equation (2.5) from a gradient flow point of view. This means that equation (2.5) is a gradient flow in the probability space embedded with a Wasserstein-2 metric. We review some facts on a formal manner; see rigorous treatment in [1].

Define the probability space on \mathbb{R}^d with finite second-order moment:

$$\mathcal{P}(\mathbb{R}^d) = \left\{ \rho(\cdot) \in C^\infty : \int_{\mathbb{R}^d} \rho(\mathbf{x}) d\mathbf{x} = 1, \int_{\mathbb{R}^d} |\mathbf{x}|^2 \rho(\mathbf{x}) d\mathbf{x} < \infty, \rho(\cdot) \geq 0 \right\}.$$

We note that $\mathcal{P}(\mathbb{R}^d)$ can be equipped with the L_2 -Wasserstein metric g_W at each $\rho \in \mathcal{P}(\mathbb{R}^d)$ to form a Riemannian manifold $(\mathcal{P}(\mathbb{R}^d), g_W)$. Let $\mathcal{F} : \mathcal{P}(\mathbb{R}^d) \rightarrow \mathbb{R}$ be an energy functional on $\mathcal{P}(\mathbb{R}^d)$. To be more precise, denote the Wasserstein gradient operator of functional $\mathcal{F}(\rho)$ at the density function $\rho \in \mathcal{P}(\mathbb{R}^d)$, such that

$$\text{grad}_W \mathcal{F}(\rho) := -\nabla \cdot \left(\rho \nabla \frac{\delta}{\delta \rho} \mathcal{F}(\rho) \right),$$

where $\frac{\delta}{\delta \rho}$ is the L_2 -first variation with respect to ρ . This yields that the gradient descent flow in the Wasserstein-2 space satisfies

$$\frac{\partial \rho}{\partial t} = -\text{grad}_W \mathcal{F}(\rho) = \nabla \cdot \left(\rho \nabla \frac{\delta}{\delta \rho} \mathcal{F}(\rho) \right).$$

206 The above PDE is also named the *Wasserstein gradient descent flow*, in short Wasser-
207 stein gradient flows, which depend on the choices of the energy functionals $\mathcal{F}(\rho)$.

208 An important example observed by [37] is as follows. Consider the relative entropy
209 functional, also named Kullback–Leibler(KL) divergence

$$210 \quad \mathcal{F}(\rho) := D_{\text{KL}}(\rho \|\pi) = \int_{\mathbb{R}^d} \rho(\mathbf{x}) \log \left(\frac{\rho(\mathbf{x})}{\pi(\mathbf{x})} \right) d\mathbf{x}.$$

211 One can show that the Fokker-Planck equation (2.5) is the gradient flow of the relative
212 entropy in $(\mathcal{P}(\mathbb{R}^d), g_W)$. Upon recognizing $\frac{\delta}{\delta \rho} D_{\text{KL}}(\rho \|\pi) = \log \left(\frac{\rho}{\pi} \right) + 1$, we obtain that
213 (2.5) can be expressed as

$$214 \quad (2.6) \quad \begin{aligned} \frac{\partial \rho}{\partial t} &= -\text{grad}_W D_{\text{KL}}(\rho \|\pi) = \nabla \cdot \left(\rho \nabla \log \left(\frac{\rho}{\pi} \right) \right) \\ &= \nabla \cdot (\rho \nabla \log \rho) - \nabla \cdot (\rho \nabla \log \pi) \\ &= \Delta \rho + \nabla \cdot (\rho \nabla f), \end{aligned}$$

215 where we use facts that $\rho \nabla \log \rho = \nabla \rho$ and $\nabla \log \pi = -\nabla f$.

216 We note that the gradient of the logarithm of the density function, i.e. $\nabla \log \rho$,
217 is often called the score function. The analysis of score functions are essential in
218 understanding the convergence behavior of the Fokker-Planck equation (2.5) toward
219 its invariant distribution; see related analytical studies in [28].

220 **2.2. Nesterov’s ODEs and underdamped Langevin dynamics.** Consider
221 the problem of minimizing $f : \mathbb{R}^d \rightarrow \mathbb{R}$ for some convex function f with L -Lipschitz
222 gradient. [52] proposed the following iterations:

$$223 \quad (2.7a) \quad \mathbf{x}_{k+1} = \mathbf{p}_k - h \nabla f(\mathbf{p}_k)$$

$$224 \quad (2.7b) \quad \mathbf{p}_{k+1} = \mathbf{x}_{k+1} + \gamma_k (\mathbf{x}_{k+1} - \mathbf{x}_k),$$

225 where $\gamma_k = (k-1)/(k-2)$. [52] showed that the above method converges at a rate
226 of $\mathcal{O}(k^{-2})$ instead of $\mathcal{O}(k^{-1})$ which is the convergence rate of the classical gradient
227 descent method. If f is further assumed to be m -strongly convex, then taking $h = 1/L$
228 and $\gamma_k = \frac{1-\sqrt{\kappa}}{1+\sqrt{\kappa}}$ where $\kappa = L/m$, yields a convergence rate of $\mathcal{O}(\exp(-k/\sqrt{\kappa}))$. This
229 is also considerably faster than gradient descent, which is $\mathcal{O}((1-\kappa^{-1})^k)$. [57] showed
230 that the continuous-time limit of Nesterov’s accelerated gradient method [52] satisfies
231 a second order ODE:

$$232 \quad (2.8) \quad \ddot{\mathbf{x}} + \gamma_t \dot{\mathbf{x}} + \nabla f(\mathbf{x}) = 0.$$

233 If f is a convex function, then $\gamma_t = 3/t$; if f is a m -strongly convex function, then
234 $\gamma_t = \gamma = 2\sqrt{m}$. As observed in [47], (2.8) can be formulated as a damped Hamiltonian
235 system:

$$236 \quad (2.9) \quad \begin{pmatrix} \dot{\mathbf{x}} \\ \dot{\mathbf{p}} \end{pmatrix} = \begin{pmatrix} 0 \\ -\gamma_t \mathbf{p} \end{pmatrix} + \begin{pmatrix} 0 & \mathbf{I} \\ -\mathbf{I} & 0 \end{pmatrix} \begin{pmatrix} \nabla_x H(\mathbf{x}, \mathbf{p}) \\ \nabla_p H(\mathbf{x}, \mathbf{p}) \end{pmatrix} = \begin{pmatrix} 0 & \mathbf{I} \\ -\mathbf{I} & -\gamma_t \mathbf{I} \end{pmatrix} \begin{pmatrix} \nabla_x H(\mathbf{x}, \mathbf{p}) \\ \nabla_p H(\mathbf{x}, \mathbf{p}) \end{pmatrix},$$

237 where the Hamiltonian function is defined as $H(\mathbf{x}, \mathbf{p}) = f(\mathbf{x}) + \|\mathbf{p}\|^2/2$, $\mathbf{p} \in \mathbb{R}^d$.
238 On the other hand, the underdamped Langevin dynamics for sampling $\Pi(\mathbf{x}, \mathbf{p}) \propto$
239 $\exp(-f(\mathbf{x}) - \|\mathbf{p}\|^2/2)$ is given by the system of SDE:

$$240 \quad d\mathbf{x}_t = \mathbf{p}_t dt,$$

$$241 \quad d\mathbf{p}_t = -\nabla f(\mathbf{x}_t) dt - \gamma_t \mathbf{p}_t dt + \sqrt{2\gamma_t} d\mathbf{B}_t,$$

242 where γ_t is some damping parameter, and \mathbf{B}_t is a d -dimensional standard Brownian
 243 motion. This can be reformulated as

$$244 \quad (2.10) \quad \begin{pmatrix} d\mathbf{x}_t \\ d\mathbf{p}_t \end{pmatrix} = \begin{pmatrix} 0 & \mathbf{I} \\ -\mathbf{I} & -\gamma_t \mathbf{I} \end{pmatrix} \begin{pmatrix} \nabla_x H(\mathbf{x}, \mathbf{p}) \\ \nabla_p H(\mathbf{x}, \mathbf{p}) \end{pmatrix} dt + \begin{pmatrix} 0 & 0 \\ 0 & \sqrt{2\gamma_t} \mathbf{I} \end{pmatrix} d\mathbf{B}_t,$$

245 where \mathbf{B}_t is a $2d$ -dimensional standard Brownian motion. Observe that by adding
 246 a suitable Brownian motion term (the last term on the right hand side of (2.10)) to
 247 (2.9), Nesterov's accelerated gradient method for convex optimization becomes an al-
 248 gorithm for sampling $\Pi(\mathbf{x}, \mathbf{p}) = \frac{1}{Z} \exp(-f(\mathbf{x}) - \|\mathbf{p}\|^2/2)$, where $Z := \int_{\mathbb{R}^{2d}} \exp(-f(\mathbf{x}) -$
 249 $\|\mathbf{p}\|^2/2) d\mathbf{x} d\mathbf{p} < +\infty$ is a normalization constant. Moreover, the \mathbf{x} -marginal of $\Pi(\mathbf{x}, \mathbf{p})$
 250 is simply $\pi(\mathbf{x}) = \frac{1}{Z_1} \exp(-f(\mathbf{x}))$ up to a normalizing constant $Z_1 := \int_{\mathbb{R}^{2d}} \exp(-f(\mathbf{x}) -$
 251 $\|\mathbf{p}\|^2/2) d\mathbf{x} d\mathbf{p} < +\infty$. Therefore, (2.10) can be used to sample distributions of the
 252 form $\exp(-f(\mathbf{x}))/Z_1$. We postpone the proofs in terms of Fokker-Planck equations
 253 and there invariant distributions in Proposition 2.1 and 2.2.

2.3. Primal-dual damping dynamics and Hessian driven damping dy-
namics. Recently, [67] proposed to solve an unconstrained strongly convex optimiza-
 tion problem using the PDHG method by considering the saddle point problem

$$\inf_{\mathbf{x} \in \mathbb{R}^d} \sup_{\mathbf{p} \in \mathbb{R}^d} \langle \nabla f(\mathbf{x}), \mathbf{p} \rangle - \frac{\gamma}{2} \|\mathbf{p}\|^2,$$

254 where γ is a damping parameter, and $f : \mathbb{R}^d \rightarrow \mathbb{R}$ is m -strongly convex. Note that
 255 the saddle point $(\mathbf{x}^*, \mathbf{p}^*)$ for the above inf-sup problem satisfies $\nabla f(\mathbf{x}^*) = \mathbf{p}^* = 0$.
 256 Then the primal-dual damping (PDD) algorithm [67] admits the following iterations

$$257 \quad \mathbf{p}_{k+1} = \frac{1}{1 + \tau_1 \gamma} \mathbf{p}_k + \frac{\tau_1}{1 + \tau_1 \gamma} \nabla f(\mathbf{x}_k),$$

$$258 \quad \tilde{\mathbf{p}}_{k+1} = \mathbf{p}_{k+1} + \omega(\mathbf{p}_{k+1} - \mathbf{p}_k),$$

$$259 \quad \mathbf{x}_{k+1} = \mathbf{x}_k - \tau_2 \mathbf{C}(\mathbf{x}_k) \tilde{\mathbf{p}}_{k+1},$$

260 where $\tau_1, \tau_2 > 0$ are dual and primal step sizes, $\omega > 0$ is an extrapolation parameter,
 261 and $\mathbf{C} \in \mathbb{R}^{d \times d}$ is a preconditioning positive definite matrix that could depend on \mathbf{x}_k
 262 and t . The continuous-time limit of the PDD algorithm can be obtained by letting
 263 $\tau_1, \tau_2 \rightarrow 0$ while keeping $\tau_1 \omega \rightarrow a$ for some $a > 0$. This yields a second-order ODE
 264 called the PDD flow:

$$265 \quad (2.11) \quad \ddot{\mathbf{x}} + \left(\gamma + a\mathbf{C}\nabla^2 f(\mathbf{x}) - \dot{\mathbf{C}}\mathbf{C}^{-1} \right) \dot{\mathbf{x}} + \mathbf{C}\nabla f(\mathbf{x}) = 0.$$

266 In the case when \mathbf{C} is constant, (2.11) reads

$$267 \quad (2.12) \quad \ddot{\mathbf{x}} + \left(\gamma + a\mathbf{C}\nabla^2 f(\mathbf{x}) \right) \dot{\mathbf{x}} + \mathbf{C}\nabla f(\mathbf{x}) = 0.$$

268 And when $\mathbf{C} = \mathbf{I}$, the PDD flow simplifies to

$$269 \quad (2.13) \quad \ddot{\mathbf{x}} + \gamma \dot{\mathbf{x}} + a\nabla^2 f(\mathbf{x}) \dot{\mathbf{x}} + \nabla f(\mathbf{x}) = 0.$$

270 This corresponds to the Hessian driven damping dynamic [3] when $\gamma = 2\sqrt{m}$. The ter-
 271 minology 'Hessian driven damping' comes from the Hessian term $\nabla^2 f(\mathbf{x}) \dot{\mathbf{x}}$ in (2.13),
 272 which is controlled by a constant $a \geq 0$. When $a = 0$, equation (2.13) reduces to
 273 Nesterov's ODE (2.8). As in dynamics (2.9), we can express equation (2.11) as

$$274 \quad (2.14) \quad \begin{pmatrix} \dot{\mathbf{x}} \\ \dot{\mathbf{p}} \end{pmatrix} = \begin{pmatrix} -a\mathbf{C} & \mathbf{C} \\ (\gamma a - 1)\mathbf{I} & -\gamma \mathbf{I} \end{pmatrix} \begin{pmatrix} \nabla_x H(\mathbf{x}, \mathbf{p}) \\ \nabla_p H(\mathbf{x}, \mathbf{p}) \end{pmatrix},$$

275 where as before the Hamiltonian function is $H(\mathbf{x}, \mathbf{p}) = f(\mathbf{x}) + \|\mathbf{p}\|^2/2$. Note that
 276 one of the key differences between (2.9) and (2.14) is that the top left block of the
 277 preconditioner matrix is nonzero in (2.14), which gives rise to the Hessian damping
 278 term $\nabla^2 f(\mathbf{x})\dot{\mathbf{x}}$. Throughout this paper, we focus on the dynamical system (2.14).

279 **2.4. Gradient-adjusted underdamped Langevin dynamics.** We design a
 280 sampling dynamics that resembles the PDD flow and the Hessian driven damping
 281 with stochastic perturbations by Brownian motions. Our goal is still to sample a
 282 distribution proportional to $\exp(-f(\mathbf{x}))$ for some $f: \mathbb{R}^d \rightarrow \mathbb{R}$. Let $H(\mathbf{x}, \mathbf{p}) = f(\mathbf{x}) +$
 283 $\|\mathbf{p}\|^2/2$. And denote by $\mathbf{X} = (\mathbf{x}, \mathbf{p}) \in \mathbb{R}^{2d}$. We consider the following SDE.

$$284 \quad (2.15) \quad d\mathbf{X}_t = -\mathbf{Q}\nabla H(\mathbf{X}_t)dt + \sqrt{2\text{sym}(\mathbf{Q})}d\mathbf{B}_t,$$

285 where $\mathbf{Q} \in \mathbb{R}^{2d \times 2d}$ is of the form

$$286 \quad (2.16) \quad \mathbf{Q} = \begin{pmatrix} a\mathbf{C} & -\mathbf{C} \\ \mathbf{I} & \gamma\mathbf{I} \end{pmatrix},$$

287 for some constant $a, \gamma \in \mathbb{R}$, and symmetric positive definite $\mathbf{C} \in \mathbb{R}^{d \times d}$. $\nabla H(\mathbf{X}_t) =$
 288 $(\nabla_x H(\mathbf{X}_t), \nabla_p H(\mathbf{X}_t))^T$. And $\text{sym}(\mathbf{Q}) = \frac{1}{2}(\mathbf{Q} + \mathbf{Q}^T)$ is the symmetrization of \mathbf{Q} . We
 289 assume that $\text{sym}(\mathbf{Q})$ is positive semidefinite.

290 Throughout this paper, we will limit our discussion to $a, \gamma \geq 0$. \mathbf{B}_t is a $2d$ -
 291 dimensional standard Brownian motion. Observe that when $a = 0$, (2.15) reduces
 292 to underdamped Langevin dynamics (2.10). When $a > 0$, (2.15) has an additional
 293 gradient term $a\mathbf{C}\nabla f(\mathbf{x}_t)$ in the $d\mathbf{x}_t$ equation. Thus, we call (2.15) gradient-adjusted
 294 underdamped Langevin dynamics. Let us examine the probability density function
 295 $\rho(\mathbf{X}, t)$ of the diffusion governed by (2.15). This is described by the following Fokker-
 296 Planck equation:

$$297 \quad (2.17) \quad \frac{\partial \rho}{\partial t} = \nabla \cdot (\mathbf{Q}\nabla H\rho) + \sum_{i,j=1}^{2d} \frac{\partial^2}{\partial X_i \partial X_j} (Q_{ij}\rho).$$

298 We assume that f is differentiable and ∇f is a smooth Lipschitz vector field. This
 299 ensures that the Fokker-Planck equation (2.17) has a smooth solution when $t > 0$ for
 300 a given initial condition, such that $\rho(\mathbf{X}, 0) \geq 0$ and $\int_{\mathbb{R}^{2d}} \rho(\mathbf{X}, 0)d\mathbf{X} = 1$.

301 Denote by $\Pi(\mathbf{X}) = \frac{1}{Z}e^{-H(\mathbf{X})}$, where Z is a normalization constant such that
 302 $\Pi(\mathbf{X})$ integrates to one on \mathbb{R}^{2d} . We show that $\Pi(\mathbf{X})$ is the stationary distribution of
 303 (2.17). First, we have the following decomposition for (2.17).

304 **PROPOSITION 2.1** ([28] Proposition 1). *The Fokker-Planck equation (2.17) can*
 305 *be decomposed as*

$$306 \quad (2.18) \quad \frac{\partial \rho}{\partial t} = \nabla \cdot \left(\rho \text{sym}(\mathbf{Q}) \nabla \log \frac{\rho}{\Pi} \right) + \nabla \cdot (\rho \Gamma),$$

307 where

$$308 \quad (2.19) \quad \begin{aligned} \Gamma(\mathbf{X}) &:= \text{sym}(\mathbf{Q}) \nabla \log(\Pi(\mathbf{X})) + \mathbf{Q} \nabla H(\mathbf{X}) \\ &= \frac{1}{2}(\mathbf{Q} - \mathbf{Q}^T) \nabla H(\mathbf{X}). \end{aligned}$$

309 In particular, the following equality holds:

$$310 \quad \nabla \cdot (\Pi(\mathbf{X})\Gamma(\mathbf{X})) = 0.$$

311 The proof is presented in Appendix C. Observe that the first term on the right-hand
 312 side of (2.18) is a Kullback–Leibler (KL) divergence functional that appears in a
 313 Fokker-Planck equation associated with the overdamped Langevin dynamics (2.5).
 314 The second term is due to the fact that the drift term $-\mathbf{Q}\nabla H$ in (2.15) is a non-
 315 gradient vector field.

316 **PROPOSITION 2.2.** $\Pi(\mathbf{X})$ is a stationary distribution for (2.17).

317 The proof is based on a straightforward calculation: When $\rho = \Pi$, we have $\nabla \cdot (\rho\Gamma) = 0$,
 318 and therefore $\frac{\partial \rho}{\partial t} = 0$. For completeness, we have included this calculation in Appen-
 319 dix C. This shows that $\Pi(\mathbf{X})$ is indeed the stationary distribution of (2.17). Like
 320 the underdamped Langevin dynamics, the \mathbf{x} -marginal of the stationary distribution
 321 is $\exp(-f(\mathbf{x}))$ up to some normalization constant. Therefore, (2.15) can be used for
 322 sampling $\frac{1}{Z_1} \exp(-f(\mathbf{x}))$ by first jointly sampling $\mathbf{X} = (\mathbf{x}, \mathbf{p})$ and then taking out the
 323 \mathbf{x} -marginal.

324 *Remark 2.3.* GAUL can also be viewed as a preconditioned overdamped Langevin
 325 dynamics on the space of $(\mathbf{x}, \mathbf{p}) \in \mathbb{R}^{2d}$. Designing optimal preconditioning matrix
 326 and optimal diffusion matrix have been studied in literature; see [11, 6, 32, 39, 33,
 327 14, 41, 40]. In particular, [41] considered the necessary condition on the optimal
 328 diffusion coefficient by studying the spectral gap of the generator associated with the
 329 SDE, which requires the solution to an optimization subproblem. While the problem
 330 considered by [41] is more general, our diffusion matrix (2.16) is much simpler and
 331 does not require solving an optimization problem. Another closely related work is
 332 [40], which considered preconditioning of the form $\mathbf{Q} = \mathbf{I} + \mathbf{J}$. Here \mathbf{I} is the identity
 333 matrix and \mathbf{J} is skew-symmetric, i.e. $\mathbf{J} = -\mathbf{J}^T$. [40] studied the optimal \mathbf{J} when the
 334 potential f is a quadratic function, which is also the focus of this work.

335 *Remark 2.4.* In [42], the authors also studied (1.3) with $\mathbf{C} = \mathbf{I}$ which they called
 336 Hessian-Free High-Resolution (HFHR) dynamics. They considered potential functions
 337 f that are L -smooth and m -strongly convex. They proved a convergence rate of
 338 $\frac{\sqrt{m}}{2\sqrt{\kappa}}$ in continuous time in terms of Wasserstein-2 distance between the target and
 339 sample measure. [42] used the randomized midpoint method [55] combined with as
 340 their discretization and showed an iteration complexity of $\tilde{\mathcal{O}}(\sqrt{d}/\varepsilon)$. Specifically,
 341 [42] showed that for a two-dimensional Gaussian target measure, under the optimal
 342 choice of parameter (damping parameter γ and step size h) for underdamped Langevin
 343 dynamics with Euler-Maruyama discretization, the convergence rate is $\mathcal{O}((1 - \kappa^{-1})^k)$.
 344 This rate is recovered in Corollary 3.17. On the other hand, [42] showed that under
 345 their choice of parameter for HRHF, the convergence rate is $\mathcal{O}((1 - 2\kappa^{-1})^k)$, which is
 346 a slight improvement compared with underdamped Langevin dynamics. In this work,
 347 we performed a detailed eigenvalue analysis of GAUL on Gaussian target measure.
 348 We showed that under our choice of parameters (γ, a, h) , the convergence rate towards
 349 the biased target measure is $\mathcal{O}((1 - c\sqrt{\kappa})^k)$ for some constant c .

350 **3. Analysis of GAUL on quadratic potential functions.** In this section,
 351 we establish the convergence rate for the proposed SDE (2.17) towards the target
 352 distribution following a Gaussian distribution.

353 **3.1. Problem set-up.** In this subsection, we present the main problem ad-
 354 dressed in this paper. We are interested in sampling from a distribution whose prob-
 355 ability density function is proportional to $\exp(-f(\mathbf{x}))$ for $f : \mathbb{R}^d \rightarrow \mathbb{R}$. In this paper,
 356 we focus on a concrete example in which the potential function f is quadratic, and

357 thus the target distribution is a Gaussian distribution. Let

$$358 \quad (3.1) \quad f(\mathbf{x}) = \frac{1}{2} \mathbf{x}^T \Sigma_*^{-1} \mathbf{x},$$

359 where $\mathbf{x} \in \mathbb{R}^d$ and $\Sigma_* \succ 0$ is a symmetric positive definite matrix in $\mathbb{R}^{d \times d}$. Define

$$360 \quad (3.2) \quad \tilde{\Sigma} = \begin{pmatrix} \Sigma_* & 0 \\ 0 & \mathbf{I} \end{pmatrix}.$$

361 As in the previous section, denote by $\mathbf{X} = (\mathbf{x}, \mathbf{p}) \in \mathbb{R}^{2d}$. And $H(\mathbf{X}) = f(\mathbf{x}) + \|\mathbf{p}\|^2/2$.
362 Then, we can write

$$363 \quad (3.3) \quad H(\mathbf{X}) = \frac{1}{2} \mathbf{X}^T \begin{pmatrix} \Sigma_*^{-1} & 0 \\ 0 & \mathbf{I} \end{pmatrix} \mathbf{X} := \frac{1}{2} \mathbf{X}^T \tilde{\Sigma}^{-1} \mathbf{X}.$$

364 Define the target density $\pi : \mathbb{R}^{2d} \rightarrow \mathbb{R}$ to be

$$365 \quad (3.4) \quad \Pi(\mathbf{X}) = \frac{1}{Z} \exp(-H(\mathbf{X})),$$

366 where $H(\mathbf{X})$ is given by (3.3) and $Z = \int_{\mathbb{R}^{2d}} \exp(-H(\mathbf{X})) d\mathbf{X}$ is a normalization con-
367 stant such that $\Pi(\mathbf{X})$ integrates to one on \mathbb{R}^{2d} . We also define the \mathbf{x} -marginal target
368 density to be

$$369 \quad (3.5) \quad \pi(\mathbf{x}) = \frac{1}{Z_1} \exp(-f(\mathbf{x})),$$

370 where $f(\mathbf{x})$ is given by (3.1) and $Z_1 = \int_{\mathbb{R}^d} \exp(-f(\mathbf{x})) d\mathbf{x}$ is a normalization constant.

Remark 3.1. Note that for any symmetric positive definite Σ_* , we have that $\Sigma_*^{-1} = \mathbf{P} \Lambda \mathbf{P}^T$ for some orthogonal matrix \mathbf{P} and diagonal matrix $\Lambda = \text{diag}(s_1, \dots, s_d)$ with $s_1 \geq \dots \geq s_d > 0$. By a change of variable $\mathbf{y} = \mathbf{P}^T \mathbf{x}$, one can rewrite $f(\mathbf{x})$ in terms of \mathbf{y} , such that

$$f(\mathbf{x}) = \frac{1}{2} \mathbf{x}^T \Sigma_*^{-1} \mathbf{x} = \frac{1}{2} \mathbf{x}^T \mathbf{P} \Lambda \mathbf{P}^T \mathbf{x} = \frac{1}{2} \mathbf{y}^T \Lambda \mathbf{y}.$$

371 For simplicity of notation, we assume that $\mathbf{P} = \mathbf{I}$ and $\Sigma_*^{-1} = \Lambda$ is a diagonal matrix.
372 We denote by $\kappa = s_1/s_d$ the condition number of f . We will also assume that
373 $s_1 > 1 > s_d$ throughout this paper. Furthermore, to simplify our analysis, we consider
374 $\mathbf{C} = \text{diag}(c_1, \dots, c_d)$.

375 **3.2. Continuous time analysis.** In this subsection, we study the convergence
376 of GAUL. In particular, we analyze the convergence of the Fokker-Planck equation
377 (2.17) to the target density (3.4), (3.5) by directly studying an ODE system of the
378 covariance of the distribution.

379 **PROPOSITION 3.2.** *Let \mathbf{X}_t be the solution of (2.15) where $H(\mathbf{X})$ is given by (3.3),
380 and $\mathbf{X}_0 \sim \mathcal{N}(0, \mathbf{I}_{2d \times 2d})$. Then $\mathbf{X}_t \sim \mathcal{N}(0, \Sigma(t))$ where the covariance $\Sigma(t)$ satisfies
381 the following matrix ODE:*

$$382 \quad (3.6) \quad \dot{\Sigma}(t) = 2 \text{sym}(\mathbf{Q}(\mathbf{I} - \tilde{\Sigma}^{-1} \Sigma(t))).$$

383 *Moreover, equation (3.6) is well-defined, and has a solution for all $t \geq 0$, such that
384 $\Sigma(t)$ is symmetric semi-positive definite.*

The proof is postponed in Appendix C. We denote by $\Sigma_{ij}(t) \in \mathbb{R}^{d \times d}$ the block components of $\Sigma(t) \in \mathbb{R}^{2d \times 2d}$:

$$\Sigma(t) = \begin{pmatrix} \Sigma_{11}(t) & \Sigma_{12}(t) \\ \Sigma_{12}^T(t) & \Sigma_{22}(t) \end{pmatrix}.$$

385 Then we can write (3.6) in terms of the block components.

386 **COROLLARY 3.3.** *The componentwise covariance matrix $\Sigma_{ij}(t)$ satisfies the fol-*
387 *lowing ODE system*

388 (3.7a) $\dot{\Sigma}_{11} = -2a(\text{sym}(\mathbf{C}\Sigma_*^{-1}\Sigma_{11}) - \mathbf{C}) + 2\text{sym}(\mathbf{C}\Sigma_{12}),$

389 (3.7b) $\dot{\Sigma}_{22} = -2\text{sym}(\Sigma_*^{-1}\Sigma_{12}) - 2\gamma(\Sigma_{22} - \mathbf{I}),$

390 (3.7c) $\dot{\Sigma}_{12} = -a\mathbf{C}\Sigma_*^{-1}\Sigma_{12} - (\mathbf{C} - \mathbf{C}\Sigma_{22}) + (\mathbf{I} - \Sigma_{11}\Sigma_*^{-1}) - \gamma\Sigma_{12},$

391 *Moreover, with initial conditions $\Sigma_{11}(0) = \Sigma_{22}(0) = \mathbf{I}$ and $\Sigma_{12}(0) = 0$, the stationary*
392 *states of $\Sigma_{11}(t)$, $\Sigma_{22}(t)$ and $\Sigma_{12}(t)$ are given by Σ_* , \mathbf{I} and 0 respectively.*

393 From now on, we consider $\mathbf{C} = \mathbf{I}$ in our analysis. We address our results for $\mathbf{C} \neq \mathbf{I}$
394 in Remark 3.10 and Remark 3.19. Note that when $\mathbf{C} = \mathbf{I}$, we have $\mathbf{Q} = \text{sym}(\mathbf{Q})$
395 is always positive semidefinite for $a, \gamma \geq 0$. Our next theorem makes sure that the
396 stationary state of equation (3.6) is actually unique and characterizes the convergence
397 speed of the covariance matrix towards its stationary state.

398 **THEOREM 3.4.** *Let \mathbf{X}_t be the solution of (2.15) where $H(\mathbf{X})$ is given by (3.3),*
399 *and $\mathbf{X}_0 \sim \mathcal{N}(0, \mathbf{I}_{2d \times 2d})$. Then $\Sigma(t)$ converges to the unique stationary state $\tilde{\Sigma}$ given*
400 *in (3.2). The optimal choice of γ is given by $\gamma^* = as_d + 2\sqrt{s_d}$ under which we have*
401 *$\|\Sigma_{11}(t) - \Sigma_*\|_{\text{F}} = \mathcal{O}(te^{-(2as_d + 2\sqrt{s_d})t})$ and $\|\Sigma_{22}(t) - \mathbf{I}\|_{\text{F}} = \mathcal{O}(te^{-(2as_d + 2\sqrt{s_d})t})$ for*
402 *$t \geq 1$.*

403 *Proof.* As mentioned in Remark 3.1, we consider $\Sigma_*^{-1} = \Lambda$. By our assumption
404 on \mathbf{X}_0 , (3.7) implies that $\Sigma_{11}(t)$, $\Sigma_{22}(t)$ and $\Sigma_{12}(t)$ will be diagonal matrices for all
405 $t > 0$. This simplifies the ODE system (3.7). After some manipulation, we obtain

(3.8)

$$406 \begin{pmatrix} \dot{\Sigma}_{11} \\ \dot{\Sigma}_{22} \\ \dot{\Sigma}_{22} \end{pmatrix} = \underbrace{\begin{pmatrix} -2a\mathbf{C}\Sigma_*^{-1} & -2\gamma\mathbf{C}\Sigma_* & -\mathbf{C}\Sigma_* \\ 0 & 0 & \mathbf{I} \\ 2\Sigma_*^{-2} & 2(-1 - a\gamma)\mathbf{C}\Sigma_*^{-1} - 2\gamma^2\mathbf{I} & -3\gamma\mathbf{I} - a\mathbf{C}\Sigma_*^{-1} \end{pmatrix}}_{\mathcal{D}} \begin{pmatrix} \Sigma_{11} \\ \Sigma_{22} \\ \dot{\Sigma}_{22} \end{pmatrix} + \mathbf{T},$$

where

$$\mathbf{T} = \begin{pmatrix} 2a\mathbf{C} + 2\gamma\mathbf{C}\Sigma_* \\ 0 \\ 2a\gamma\Sigma_*^{-1}\mathbf{C} + 2\gamma^2\mathbf{I} + 2\Sigma_*^{-1}\mathbf{C} - 2\Sigma_*^{-1} \end{pmatrix},$$

407 And $\mathbf{C} = \mathbf{I}$. We have already seen in Corollary 3.3 that the stationary state of $\Sigma(t)$
408 is $\tilde{\Sigma}$ given in (3.2). To show uniqueness, we compute the eigenvalues of \mathcal{D} :

409 $\lambda_0^{(i)} = -as_i - \gamma,$

410 $\lambda_1^{(i)} = -as_i - \gamma - \sqrt{\gamma^2 - 2a\gamma s_i + s_i(-4 + a^2 s_i)},$

411 $\lambda_2^{(i)} = -as_i - \gamma + \sqrt{\gamma^2 - 2a\gamma s_i + s_i(-4 + a^2 s_i)},$

where s_i 's are the diagonal elements of Λ for $i = 1, \dots, d$. It is clear that 0 is not an
eigenvalue of \mathcal{D} . Therefore, $\tilde{\Sigma}$ is the unique stationary state for $\Sigma(t)$. The convergence

speed of (3.8) is essentially controlled by the largest real part of the eigenvalues of \mathcal{D} . Note that for all i ,

$$\Re(\lambda_2^{(i)}) \geq \Re(\lambda_0^{(i)}) \geq \Re(\lambda_1^{(i)}),$$

where $\Re(z)$ denotes the real part of $z \in \mathbb{C}$. Therefore, to characterize the convergence speed of (3.8), it suffices to control $\max_i \Re(\lambda_2^{(i)})$. By Lemma B.7, we know that for any given $a \geq 0$, the optimal choice of γ is

$$\gamma^* = \arg \min_{\gamma > 0} \max_i \Re(\lambda_2^{(i)}) = as_d + 2\sqrt{s_d}.$$

With $\gamma = \gamma^*$, we get that

$$\max_{i,j} \Re(\lambda_j^{(i)}) \leq \max_i \Re(\lambda_2^{(i)}) \leq -2as_d - 2\sqrt{s_d}.$$

412 This leads to

$$413 \quad (3.9) \quad \left\| \begin{pmatrix} \Sigma_{11}(t) - \Sigma_* \\ \Sigma_{22}(t) - \mathbf{I} \\ \dot{\Sigma}_{22}(t) \end{pmatrix} \right\|_{\mathbb{F}} \leq C_1 t e^{-(2as_d + 2\sqrt{s_d})t}, \quad \square$$

which is valid for $t \geq 1$. The constant C_1 depends on d, s_1, s_d^{-1} at most polynomially according to Lemma B.8. Note that the extra t dependence comes from the repeated eigenvalue $\lambda_0^{(d)} = \lambda_1^{(d)} = \lambda_2^{(d)}$ when $\gamma = \gamma^*$. By a triangle inequality, we get

$$\|\Sigma_{11} - \Sigma_*\|_{\mathbb{F}} \leq \left\| \begin{pmatrix} \Sigma_{11}(t) - \Sigma_* \\ \Sigma_{22}(t) - \mathbf{I} \\ \dot{\Sigma}_{22}(t) \end{pmatrix} \right\|_{\mathbb{F}} \leq C_1 t e^{-(2as_d + 2\sqrt{s_d})t}.$$

And similarly,

$$\|\Sigma_{22} - \mathbf{I}\|_{\mathbb{F}} \leq C_1 t e^{-(2as_d + 2\sqrt{s_d})t}.$$

414 *Remark 3.5.* The choice $a = 0$ corresponds to underdamped Langevin dynamics
415 (UL). Taking $a > 0$ gives an extra factor of $e^{-2as_d t}$ in terms of convergence.

DEFINITION 3.6 (Mixing time). *The total variation between two probability measures \mathcal{P} and \mathcal{Q} over a measurable space $(\mathbb{R}^d, \mathcal{F})$ is*

$$\text{TV}(\mathcal{P}, \mathcal{Q}) = \sup_{A \in \mathcal{F}} |\mathcal{P}(A) - \mathcal{Q}(A)|.$$

Let \mathcal{T}_p be an operator on the space of probability distributions. Assume that $\mathcal{T}_p^k(\nu_0) \rightarrow \nu$ as $k \rightarrow \infty$ for some initial distribution ν_0 and stationary distribution ν . The discrete δ -mixing time ($\delta \in (0, 1)$) is given by

$$t_{\text{mix}}^{\text{dis}}(\delta; \nu_0, \nu) = \min\{k \mid \text{TV}(\mathcal{T}_p^k(\nu_0), \nu) \leq \delta\}.$$

Similarly, if $\mathcal{T}_p(t; \cdot)$ is an operator for each $t \geq 0$ with $\mathcal{T}_p(0; \cdot) = \text{id}(\cdot)$ and assume that $\mathcal{T}_p(t; \nu_0) \rightarrow \nu$ as $t \rightarrow \infty$. The continuous δ -mixing time ($\delta \in (0, 1)$) is given by

$$t_{\text{mix}}^{\text{cont}}(\delta; \nu_0, \nu) = \min\{t \mid \text{TV}(\mathcal{T}_p(t; \nu_0), \nu) \leq \delta\}.$$

THEOREM 3.7 ([24]). Let $\mu \in \mathbb{R}^d$, Σ_1, Σ_2 be two positive definite covariance matrices, and $\lambda_1, \dots, \lambda_d$ denote the eigenvalues of $\Sigma_1^{-1}\Sigma_2 - \mathbf{I}$. Then the total variation satisfies

$$\text{TV}(\mathcal{N}(\mu, \Sigma_1), \mathcal{N}(\mu, \Sigma_2)) \leq \frac{3}{2} \min \left\{ 1, \sqrt{\sum_{i=1}^d \lambda_i^2} \right\}.$$

416 A straightforward corollary follows from Schur decomposition theorem.

COROLLARY 3.8. We have

$$\text{TV}(\mathcal{N}(\mu, \Sigma_1), \mathcal{N}(\mu, \Sigma_2)) \leq \frac{3}{2} \min \{1, \|\Sigma_1^{-1}\Sigma_2 - \mathbf{I}\|_{\text{F}}\}.$$

417 Using Theorem 3.4 and Corollary 3.8, we obtain the following mixing time theorem
418 when the potential function f is quadratic.

THEOREM 3.9 (Continuous mixing time). Consider the same setting as in Theorem 3.4. Consider $0 < \delta \ll 1$. Then

$$t_{\text{mix}}^{\text{cont}}(\delta; \nu_0, \pi) \leq \frac{\mathcal{O}(\log(d) + \log(\kappa)) + \log(1/\delta)}{as_d + 2\sqrt{s_d}}.$$

419 Here ν_0 is the distribution of \mathbf{x} , which is $\mathcal{N}(0, \mathbf{I}_{d \times d})$. π is the target density in the \mathbf{x}
420 variable given in (3.5).

Proof. We shall use Corollary 3.8 with

$$\Sigma_1 = \Sigma_*, \quad \Sigma_2 = \Sigma_{11}(t).$$

421 We have

$$\begin{aligned} 422 \quad \|\Sigma_1^{-1}\Sigma_2 - \mathbf{I}\|_{\text{F}} &= \|\Sigma_*^{-1}(\Sigma_{11}(t) - \Sigma_*)\|_{\text{F}} \\ 423 \quad &\leq C_1 t e^{-(2as_d + 2\sqrt{s_d})t} s_1. \end{aligned}$$

424 By a direct computation, we get

$$425 \quad t_{\text{mix}}^{\text{cont}}(\delta; \nu_0, \pi) \leq \frac{\log(\tilde{C}_1/\delta)}{as_d + 2\sqrt{s_d}}, \quad \square$$

where $\tilde{C}_1 = \frac{3}{2}C_1s_1$. By Lemma B.8, we have that

$$t_{\text{mix}}^{\text{cont}}(\delta; \nu_0, \pi) \leq \frac{\mathcal{O}(\log(d\kappa)) + \log(1/\delta)}{as_d + 2\sqrt{s_d}}.$$

Remark 3.10. When $\mathbf{C} = \text{diag}(c_1, \dots, c_d)$ and $\text{sym}(\mathbf{Q}) \succeq 0$ in (2.16), our proof can be easily adapted to show similar results in Theorem 3.9:

$$t_{\text{mix}}^{\text{cont}}(\delta; \nu_0, \pi) \leq \frac{\mathcal{O}(\log(d) + \log(\hat{\kappa})) + \log(1/\delta)}{a\hat{s}_d + 2\sqrt{\hat{s}_d}},$$

426 where \hat{s}_i is the i -th largest eigenvalue of matrix $\mathbf{C}\Sigma_*^{-1}$. And $\hat{\kappa} = \hat{s}_1/\hat{s}_d$. In other
427 words, the matrix \mathbf{C} can be viewed as a preconditioner for the target covariance
428 matrix in the sampling problem.

429 **3.3. Discrete time analysis.** To implement (2.15), we need to consider its time
 430 discretization. As discretization is not the focus of this paper, we will only analyze
 431 the simplest discretization using the Euler-Maruyama method in Appendix A.

432 Let us first make a few observations regarding the discretization in Appendix A.
 433 After a straightforward computation, we obtain the following update rule.

434 **PROPOSITION 3.11.** *The Euler-Maruyama discretization of (2.15) given in Ap-*
 435 *pendix A with step size h can be written in the following form*

$$436 \quad (3.10) \quad \begin{pmatrix} \mathbf{x}_{n+1} \\ \mathbf{p}_{n+1} \end{pmatrix} = \mathbf{A} \begin{pmatrix} \mathbf{x}_n \\ \mathbf{p}_n \end{pmatrix} + \mathbf{L}\mathbf{z},$$

437 where

$$438 \quad (3.11) \quad \mathbf{A} = \underbrace{\mathbf{I}_{2d \times 2d} - h \begin{pmatrix} a\Lambda & -\mathbf{I}_{d \times d} \\ \Lambda & \gamma \mathbf{I}_{d \times d} \end{pmatrix}}_{\mathbf{G}}, \quad \mathbf{L} = \begin{pmatrix} \sqrt{2ah}\mathbf{I} & 0 \\ 0 & \sqrt{2\gamma h}\mathbf{I} \end{pmatrix}.$$

439 And \mathbf{z} is a 2d-dimensional Brownian motion, i.e., $\mathbf{z} \sim \mathcal{N}(0, \mathbf{I}_{2d \times 2d})$.

440 Using (3.10), we can derive the evolution of the mean and covariance at each time
 441 step. As before, let us denote by $\mathbf{X}_n = (\mathbf{x}_n, \mathbf{p}_n)$.

COROLLARY 3.12. *Suppose that $\mathbb{E}(\mathbf{x}_0) = \mathbb{E}(\mathbf{p}_0) = 0$. Then*

$$\text{cov}(\mathbf{X}_{n+1}, \mathbf{X}_{n+1}) = \mathbf{A} \text{cov}(\mathbf{X}_n, \mathbf{X}_n) \mathbf{A}^T + \mathbf{L}\mathbf{L}^T.$$

442 *Proof.* From (3.10), it is clear that $\mathbb{E}(\mathbf{x}_n) = \mathbb{E}(\mathbf{p}_n) = 0$ for all $n \geq 0$. We calculate

$$443 \quad \text{cov}(\mathbf{X}_{n+1}, \mathbf{X}_{n+1}) = \mathbb{E}(\mathbf{A}\mathbf{X}_n\mathbf{X}_n^T\mathbf{A}^T + \mathbf{A}\mathbf{X}_n\mathbf{z}^T\mathbf{L}^T + \mathbf{L}\mathbf{z}\mathbf{X}_n^T\mathbf{A}^T + \mathbf{L}\mathbf{z}\mathbf{z}^T\mathbf{L}^T)$$

$$444 \quad = \mathbf{A} \text{cov}(\mathbf{X}_n, \mathbf{X}_n) \mathbf{A}^T + \mathbf{L}\mathbf{L}^T. \quad \square$$

COROLLARY 3.13. *Denote by \mathbf{Y}^* a solution to the fixed point equation $\mathbf{Y} = \mathbf{A}\mathbf{Y}\mathbf{A}^T + \mathbf{L}\mathbf{L}^T$. And let $\mathbf{Y}_n = \text{cov}(\mathbf{X}_n, \mathbf{X}_n) - \mathbf{Y}^*$. Then*

$$\mathbf{Y}_{n+1} = \mathbf{A}\mathbf{Y}_n\mathbf{A}^T.$$

THEOREM 3.14. *Suppose $a \geq \frac{2}{\sqrt{s_1} - \sqrt{s_d}}$ and the step size h satisfies $0 < h < 1/(as_1 + \gamma)$ and $\gamma = \gamma^* = as_d + 2\sqrt{s_d}$. Then there exists a unique \mathbf{Y}^* satisfying*

$$\mathbf{Y}^* = \mathbf{A}\mathbf{Y}^*\mathbf{A}^T + \mathbf{L}\mathbf{L}^T.$$

445 *Moreover, the iteration $\mathbf{Y}_{k+1} = \mathbf{A}\mathbf{Y}_k\mathbf{A}^T + \mathbf{L}\mathbf{L}^T$ converges to \mathbf{Y}^* linearly: $\|\mathbf{Y}_k - \mathbf{Y}^*\|_{\text{F}} \leq \tilde{C}h^2k^2(1 - \frac{h}{2}(as_d + \sqrt{s_d}))^{2k-2}$, where the constant $\tilde{C} = d^2 \cdot \mathcal{O}(\text{poly}(\kappa))$.*

447 *Proof.* Existence: we directly compute this stationary point in Lemma B.17.
 448 Uniqueness: by Lemma B.14 and Corollary B.10 we see that \mathbf{Y}^* is unique. The
 449 convergence rate is proved in Lemma B.14 and Theorem B.16.

450 **THEOREM 3.15 (Discrete mixing time).** *Suppose $\sqrt{s_1} - \sqrt{s_d} \geq 2$. We take $a = 1$,*
 451 *$\gamma = \gamma^* = s_d + 2\sqrt{s_d}$, $h = 1/5s_1$. If we use the Euler-Maruyama scheme for (2.15),*
 452 *then for $0 < \delta \ll 1$,*

$$453 \quad (3.12) \quad t_{\text{mix}}^{\text{dis}}(\delta; \nu_0, \tilde{\pi}) = \mathcal{O} \left(\frac{\log(\kappa) + \log(1/\delta) + \log(d)}{\frac{1}{\kappa} + \frac{1}{\sqrt{\kappa s_1}}} \right).$$

454 Here ν_0 is the distribution of \mathbf{x} , which is $\mathcal{N}(0, \mathbf{I}_{d \times d})$. $\tilde{\pi}$ is the target density in the \mathbf{x}
 455 variable which is a zero mean Gaussian distribution with a variance given by (B.24).

Proof. Note that from our previous notation, we have that

$$\text{cov}(\mathbf{x}_k, \mathbf{x}_k) = \begin{pmatrix} \mathbf{I}_{d \times d} & 0 \\ 0 & 0 \end{pmatrix} \text{cov}(\mathbf{X}_k, \mathbf{X}_k) \begin{pmatrix} \mathbf{I}_{d \times d} \\ 0 \end{pmatrix} =: \tilde{\mathbf{Y}}_k.$$

Moreover, let us define

$$\tilde{\mathbf{Y}}^* = \begin{pmatrix} \mathbf{I}_{d \times d} & 0 \\ 0 & 0 \end{pmatrix} \mathbf{Y}^* \begin{pmatrix} \mathbf{I}_{d \times d} \\ 0 \end{pmatrix}$$

456 to be the limiting covariance in the \mathbf{x} variable for the discretization (\mathbf{Y}^* is defined in
457 Theorem 3.14). Clearly, we have that

$$458 \quad (3.13) \quad \|\tilde{\mathbf{Y}}_k - \tilde{\mathbf{Y}}^*\|_{\text{F}} \leq \|\mathbf{Y}_k - \mathbf{Y}^*\|_{\text{F}} \leq \tilde{C} h^2 k^2 \left(1 - \frac{h}{2}(as_d + \sqrt{s_d})\right)^{2k-2}.$$

459 Using Corollary 3.8, we compute

$$460 \quad \begin{aligned} \|(\tilde{\mathbf{Y}}^*)^{-1} \tilde{\mathbf{Y}}_k - \mathbf{I}\|_{\text{F}} &= \|(\tilde{\mathbf{Y}}^*)^{-1} (\tilde{\mathbf{Y}}_k - \tilde{\mathbf{Y}}^*)\|_{\text{F}} \\ 461 \quad &\leq \|(\tilde{\mathbf{Y}}^*)^{-1}\|_{\text{F}} \|\tilde{\mathbf{Y}}_k - \tilde{\mathbf{Y}}^*\|_{\text{F}}. \end{aligned}$$

462 By Lemma B.17, $\tilde{\mathbf{Y}}^*$ is a diagonal matrix. Therefore $(\tilde{\mathbf{Y}}^*)^{-1}$ is also a diagonal matrix.
463 Moreover, from (B.24), we see that $\|(\tilde{\mathbf{Y}}^*)^{-1}\|_{\text{F}} \leq \sqrt{d} \mathcal{O}(\text{poly}(\kappa))$. Therefore, we obtain

$$464 \quad \begin{aligned} \|(\tilde{\mathbf{Y}}^*)^{-1} \tilde{\mathbf{Y}}_k - \mathbf{I}\|_{\text{F}} &\leq d^{5/2} \cdot \mathcal{O}(\text{poly}(\kappa)) h^2 k^2 \left(1 - \frac{h}{2}(s_d + \sqrt{s_d})\right)^{2k-2} \\ 465 \quad &\leq d^{5/2} \cdot \mathcal{O}(\text{poly}(\kappa)) h^2 k^2 e^{-(k-1)h(s_d + \sqrt{s_d})}, \quad \square \end{aligned}$$

where we used $1 - x \leq e^{-x}$ for $x \in \mathbb{R}$ to get the second inequality. Letting $h = 1/5s_1$ and taking logarithm on both hand sides, we conclude that

$$t_{\text{mix}}^{\text{dis}}(\delta; \nu_0, \tilde{\pi}) \leq \frac{\mathcal{O}(\log(d)) + \mathcal{O}(\log(\kappa)) + \log(1/\delta)}{\frac{1}{10} \left(\frac{1}{\kappa} + \frac{1}{\sqrt{\kappa s_1}}\right)}.$$

466 **THEOREM 3.16** (A better choice of a). *The denominator of the mixing time given*
467 *in Theorem 3.15 can be improved to $\kappa^{-1/2}$ by choosing $a = \frac{2}{\sqrt{s_1 - \sqrt{s_d}}}$, $\gamma = as_d + 2\sqrt{s_d}$*
468 *and $h = \frac{1}{2(as_1 + \gamma)}$. To be more precise, we have*

$$469 \quad (3.14) \quad t_{\text{mix}}^{\text{dis}}(\delta; \nu_0, \tilde{\pi}) = \mathcal{O} \left(\frac{\log(\kappa) + \log(1/\delta) + \log(d)}{\frac{1}{\sqrt{\kappa}}} \right).$$

470 *Proof.* The proof will be very similar to that of Theorem 3.15. We start with
471 (3.13). And we can explicitly calculate

$$472 \quad \begin{aligned} 1 - \frac{h}{2}(as_d + \sqrt{s_d}) &= 1 - \frac{as_d + \sqrt{s_d}}{4(as_1 + as_d + 2\sqrt{s_d})} \\ 473 \quad &= 1 - \frac{2s_d + \sqrt{s_d}(\sqrt{s_1} - \sqrt{s_d})}{8(s_1 + s_d + \sqrt{s_d}(\sqrt{s_1} - \sqrt{s_d}))} \\ 474 \quad &= 1 - \frac{\sqrt{s_1 s_d} + s_d}{8(s_1 + \sqrt{s_1 s_d})} \\ 475 \quad &\leq 1 - \frac{1}{16\sqrt{\kappa}}. \end{aligned}$$

476 The rest of the proof is the same as the proof of Theorem 3.15 and we will suppress
477 it for brevity. \square

478 The following corollary follows from Lemma B.15 and the proof of Theorem 3.15.

479 **COROLLARY 3.17** (Underdamped Langevin mixing time). *Suppose $a = 0$, $\gamma =$*
 480 *$2\sqrt{s_d}$, $h = \sqrt{s_d}/s_1$. If we use the Euler-Maruyama scheme for (2.15), then for $0 <$*
 481 *$\delta \ll 1$,*

$$482 \quad (3.15) \quad t_{\text{mix}}^{\text{dis}}(\delta; \nu_0, \tilde{\pi}) = \mathcal{O}\left(\frac{\log(\kappa) + \log(1/\delta) + \log(d)}{\frac{1}{\kappa}}\right),$$

483 ν_0 is the distribution of \mathbf{x} , which is $\mathcal{N}(0, \mathbf{I}_{d \times d})$. $\tilde{\pi}$ is the target density in the \mathbf{x}
 484 variable which is a zero mean Gaussian with variance given by (B.24) with $a = 0$.

485 *Remark 3.18.* $a = 0$ in (2.15) corresponds to the underdamped Langevin dynam-
 486 ics. In this case, we show in Lemma B.15 that to guarantee convergence (to a biased
 487 target) the step size restriction on h is more strict than when $a = 1$. In particular,
 488 when $a = 0$ it follows from Lemma B.15 that the choice $h = 1/5s_1$ does not guarantee
 489 convergence if $s_d < 10^{-2}$. Comparing (3.14) and (3.15), we see that the mixing time
 490 for GAUL beats that of underdamped Langevin dynamics under the Euler-Maruyama
 491 discretization. We are aware that this does not imply the same result will hold when
 492 comparing the mixing time towards the true target distribution $\pi(\mathbf{x})$ given in (3.5),
 493 due to the presence of bias in the Euler-Maruyama scheme. Designing better dis-
 494 cretization and reducing the bias in the stationary distribution is left as future works.

495 *Remark 3.19.* When $\mathbf{C} = \text{diag}(c_1, \dots, c_d)$ and $\text{sym}(\mathbf{Q}) \succeq 0$ in (2.16), we also have
 496 a similar mixing time described in Theorem 3.16, which is
 497 $\mathcal{O}(\sqrt{\hat{\kappa}}(\log(\hat{\kappa}) + \log(1/\delta) + \log(d)))$ when $a = \frac{2}{\sqrt{\hat{s}_1} - \sqrt{\hat{s}_d}}$, $\gamma = a\hat{s}_d + 2\sqrt{\hat{s}_d}$ and $h =$
 498 $\frac{1}{2(a\hat{s}_1 + \gamma)}$. The notation \hat{s}_i and $\hat{\kappa}$ are defined in Remark 3.10.

499 *Remark 3.20.* When the target potential f is not a quadratic function, it is more
 500 technical in proving the convergence speed. A common technique to prove convergence
 501 in the Wasserstein-2 distance is by a coupling argument (see [16, 22]). [9] proved L_2
 502 convergence under a Poincarè-type inequality using Bochner's formula. In the L_1
 503 distance and KL divergence, [28] design convergence analysis towards these problems.
 504 We leave the convergence analysis of general f with optimal choices of preconditioned
 505 matrices \mathbf{Q} in future works.

506 **4. Numerical experiment.** In this section, we implement several numerical
 507 examples to compare the proposed SDE with the overdamped (labeled 'ol') and un-
 508 derdamped (labeled 'ul') Langevin dynamics. We use the same step size for all three
 509 algorithms. Recall that 'ol' corresponds to the choice $a = 1, \gamma = 0$ and 'ul' corresponds
 510 to $a = 0$ in (2.15). We set $\mathbf{C} = \mathbf{I}$.

511 4.1. Gaussian examples.

512 **4.1.1. One dimension.** We begin with a simple example, a one dimensional
 513 Gaussian distribution with zero mean. In Figure 1, we consider two cases where the
 514 variances are given by 0.01 and 100 respectively. We first sample $M = 10^5$ particles
 515 from $\mathcal{N}(0, \mathbf{I}_{2 \times 2})$ (although our experiment is in one dimension, we need both \mathbf{x} and \mathbf{p}
 516 variables). When measuring the convergence speed, we use KL divergence in Gaussian
 517 distributions to measure the change of covariances. Note that we will only measure
 518 the KL divergence in the x variable, since we are primarily interested in sampling
 519 distribution of the form $\frac{1}{2}e^{-f(x)}$. In this experiment, we can make use of the fact
 520 that the sample distribution and the target distribution are both Gaussians. And the

521 KL divergence between two centered Gaussians has a closed form expression:

$$522 \quad (4.1) \quad D_{\text{KL}}(\Sigma(t), \tilde{\Sigma}) = \frac{1}{2} \left(\text{tr}(\Sigma(t)\tilde{\Sigma}^{-1}) - \log \det(\Sigma(t)\tilde{\Sigma}^{-1}) - d \right).$$

523 In this one dimensional example, we study two cases where $\tilde{\Sigma} = 0.01$ or 100 .
 524 $\Sigma(t)$ can be approximated by the unbiased sample variance. For $\tilde{\Sigma} = 0.01$, we choose
 525 time step size $h = 10^{-4}$, total number of steps $N = 400$, $\gamma_{ul} = 2\tilde{\Sigma}^{-1/2} = 20$,
 526 $\gamma_{pdd} = 2\tilde{\Sigma}^{-1/2} + \tilde{\Sigma}^{-1} = 120$. For $\tilde{\Sigma} = 100$, we choose the time step size $h = 10^{-2}$,
 527 total number of steps $N = 600$, $\gamma_{ul} = 2\tilde{\Sigma}^{-1/2} = 0.2$, $\gamma_{pdd} = 2\tilde{\Sigma}^{-1/2} + \tilde{\Sigma}^{-1} = 0.21$. In
 528 Figure 1, we observe that our proposed method outperforms both overdamped and
 underdamped Langevin dynamics in both cases.

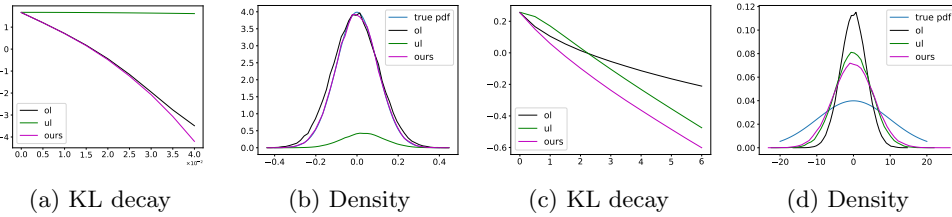


Fig. 1: Convergence and density comparisons of three methods. (a) and (c): KL divergence between the sample and the target distribution, which is a one-dimensional Gaussian with zero mean and variance 0.01 (a), 100 (c). ‘ol’ represents overdamped Langevin dynamics; ‘ul’ represents underdamped Langevin dynamics. x-axis represents time and y-axis is in \log_{10} scale. (b) and (d): density comparison at the end of the experiment between the three methods and the true density.

529

530 **4.1.2. 20 dimensions.** Let the target distribution be a 20-dimensional Gaussian
 531 with zero mean and covariance given by a diagonal matrix with entries $0.05 + 5i$ for
 532 $i = 0, \dots, 19$. The last dimension has the largest variance, which is $\sigma_{\max}^2 = 95.05$.
 533 Therefore, we choose $a = \frac{2}{\sigma_{\min}^{-1/2} - \sigma_{\max}^{-1/2}}$, $\gamma_{ul} = 2\sigma_{\max}^{-1}$ and $\gamma_{pdd} = 2\sigma_{\max}^{-1} + a\sigma_{\max}^{-2}$. In
 534 this experiment, we use (1) time step size $h = 5 \times 10^{-3}$ and run for 4000 steps; (2)
 535 time step size $h = 5 \times 10^{-2}$ and run for 400 steps. The KL divergence can still be
 536 computed using (4.1). To visualize the final distribution in a two-dimensional plane,
 537 we plot the scatter plot of the samples in the first and the last dimensions. All results
 538 are presented in Figure 2.

539 **4.2. Mixture of Gaussian.**

540 **4.2.1. Strongly log-concave.** Consider the problem of sampling from a mix-
 541 ture of Gaussian distributions $\mathcal{N}(\alpha, \mathbf{I})$ and $\mathcal{N}(-\alpha, \mathbf{I})$, whose density satisfies:

$$542 \quad p(\mathbf{x}) = \frac{1}{2(2\pi)^{d/2}} \left(e^{-\|\mathbf{x}-\alpha\|_2^2/2} + e^{-\|\mathbf{x}+\alpha\|_2^2/2} \right).$$

543 The corresponding potential is given as

$$544 \quad (4.2) \quad f(\mathbf{x}) = \frac{1}{2} \|\mathbf{x} - \alpha\|_2^2 - \log \left(1 + e^{-2\mathbf{x}^\top \alpha} \right),$$

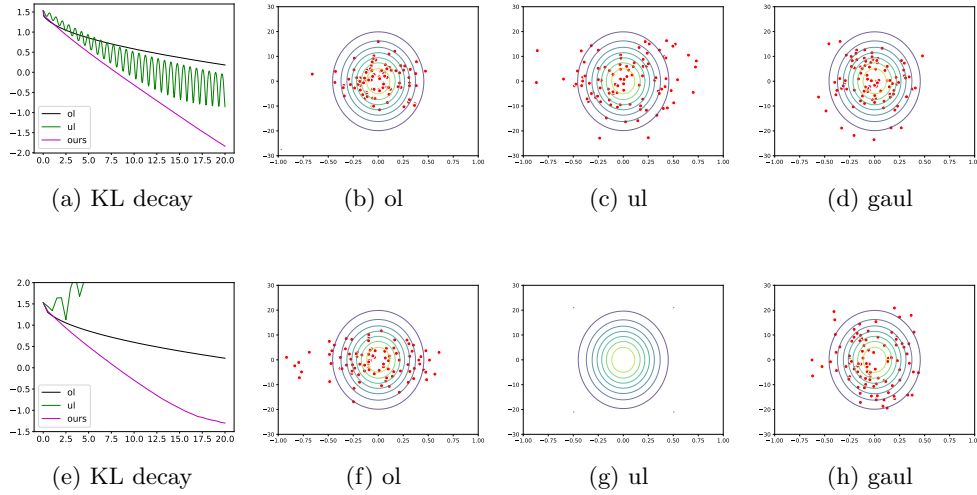


Fig. 2: Convergence and scatter plots. (a)–(d): $h = 0.005$. (e)–(h): $h = 0.05$. (a) and (e): KL divergence between the sample and target distribution. The x-axis represents time and the y-axis is in \log_{10} scale. Rest panels: scatter plot of the three methods at the end of the experiment for different step sizes. Contours of the true density are also provided for comparisons. In (g) there are no scatter points shown as ‘ul’ does not converge for this choice of h .

545

$$546 \quad (4.3) \quad \nabla f(\mathbf{x}) = \mathbf{x} - \alpha + 2\alpha(1 + e^{2\mathbf{x}^\top \alpha})^{-1}.$$

547 Following [27, 20], we set $\alpha = (1/2, 1/2)$ and $d = 2$. This choice of parameters
 548 yields strong convexity parameter $m = 1/2$ and Lipschitz constant $L = 1$. We choose
 549 $a = \frac{2}{\sqrt{L} - \sqrt{m}}$, $\gamma_{ul} = 2m^{1/2}$ and $\gamma_{pdd} = 2m^{1/2} + am$. Initially particles are sampled
 550 from $\mathcal{N}(0, \mathbf{I})$. We use time step $h = 2 \times 10^{-4}$ and run for 2000 steps. We use 5×10^5
 551 particles and $n^2 = 2500$ bins to approximate the KL divergence between the sample
 552 points and the target distribution (see Remark 4.1). The results are shown in Figure 3.
 553

554 *Remark 4.1.* To compute the KL divergence between sample points and a non-
 555 Gaussian target distribution in two dimension, we first get the 2d histogram of the
 556 samples points using n^2 bins (n in each dimension). We then use this 2d histogram as
 557 an approximation of the empirical distribution of the samples. Similarly, we can get
 558 a discretized target distribution by evaluating the target distribution at the center of
 559 each bins. Finally, we can compute the discrete KL divergence using n^2 values from
 560 the histogram and the discretized target distribution.

561 **4.2.2. Non log-concave .** We also consider the same example as in Subsec-
 562 tion 4.2.1 with $\alpha = (3, 3)$. As the distance between the two Gaussians increases, the
 563 target density is no longer log-concave. We use time step size $h = 10^{-3}$ and run for
 564 2000 steps. We use $a = 1$, $\gamma_{ul} = \sqrt{2}$, and $\gamma_{pdd} = \sqrt{2} + 1/2$. We use 5×10^5 particles
 565 and $n^2 = 2500$ bins to evaluate the KL divergence. The results are demonstrated in
 566 Figure 4.

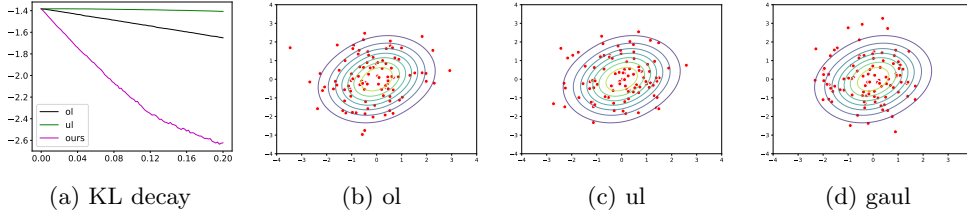


Fig. 3: Convergence and scatter plots. (a): KL divergence between the sample and target distribution, which is a mixture of two unit variance Gaussians located at $(1/2, 1/2)$ and $(-1/2, -1/2)$. x-axis represents time and y-axis is in \log_{10} scale. (b)–(d): scatter plot of the three methods at the end of the experiment. Contour of the true density is also provided for comparison.

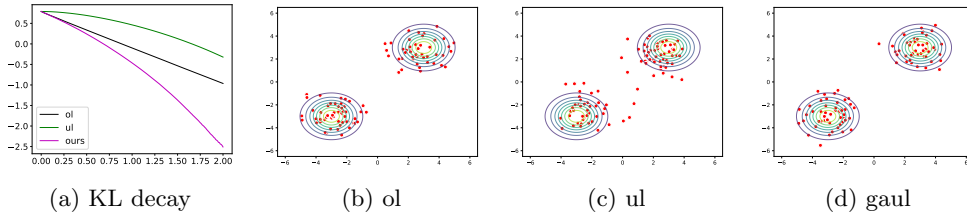


Fig. 4: Convergence and scatter plots for mixture of Gaussians centered at $(3, 3)$ and $(-3, -3)$.

4.3. Quadratic cosine. Consider a potential function given by a quadratic function and a cosine term:

$$f(\mathbf{x}) = \frac{1}{2} \mathbf{x}^T B^{-1} \mathbf{x} - \cos(\mathbf{c}^T \mathbf{x})$$

567 where $B = \mathbf{P} \text{diag}(1, 25) \mathbf{P}^T$ for an orthogonal matrix \mathbf{P} and $\mathbf{c} = \sqrt{0.95} (1, 1)^T$.
 568 Here \mathbf{P} is generated by using `torch.linalg.qr(torch.randn(d))` in Pytorch, where $d = 2$
 569 is the dimension. We set $a = 1$, $\gamma_{ul} = 2m^{1/2}$ and $\gamma_{pdd} = 2m^{1/2} + m$ where we
 570 choose $m = 1/25$. We use time step size $h = 10^{-2}$ and run for 1000 steps. We use
 571 5×10^5 particles and $n^2 = 2500$ bins to evaluate the KL divergence. The results are
 572 demonstrated in Figure 5.

4.4. Bimodal. We consider a two-dimensional bimodal distribution studied in [64] whose target density has the following form:

$$p(\mathbf{x}) \propto \exp(-2(\|\mathbf{x}\| - 3)^2) \left[\exp(-2(x_1 - 3)^2) + \exp(-2(x_1 + 3)^2) \right].$$

The corresponding potential function is given by

$$f(\mathbf{x}) = 2(\|\mathbf{x}\| - 3)^2 - 2 \log \left[\exp(-2(x_1 - 3)^2) + \exp(-2(x_1 + 3)^2) \right].$$

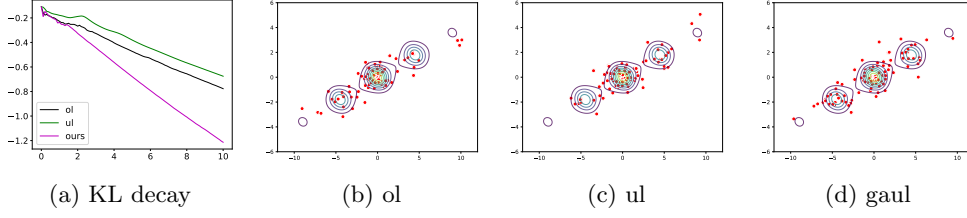


Fig. 5: Convergence and scatter plots for the quadratic cosine example.

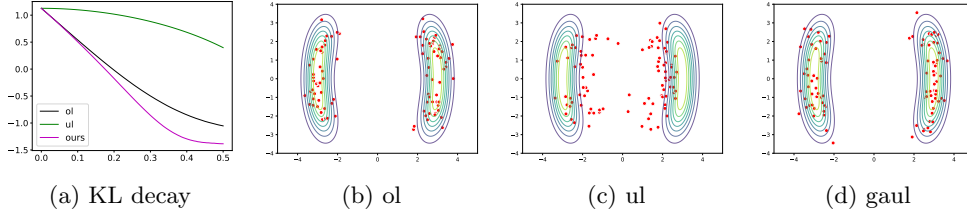


Fig. 6: Convergence and scatter plots for the bimodal example.

573 The gradient is

$$574 \quad \nabla f(\mathbf{x}) = \frac{4(x_1 - 3) \exp(-2(x_1 - 3)^2) + 4(x_1 + 3) \exp(-2(x_1 + 3)^2)}{\exp(-2(x_1 - 3)^2) + \exp(-2(x_1 + 3)^2)} \mathbf{e}_1$$

$$575 \quad + 4 \frac{(\|\mathbf{x}\| - 3)\mathbf{x}}{\|\mathbf{x}\|},$$

576 where $\mathbf{e}_1 = (1, 0)^T$ is the first standard coordinate vector. We set $\gamma_{ul} = 2m^{1/2}$ and
 577 $\gamma_{pdd} = 2m^{1/2} + m$ where we choose $m = 1/2$. We use time step size $h = 10^{-3}$ and
 578 run for 500 iterations. We use 10^6 particles and $n^2 = 2500$ bins to evaluate the KL
 579 divergence. The results are shown in Figure 6.

580 **4.5. Bayesian logistic regression.** We consider the Bayesian logistic regression
 581 problem studied in [27, 20, 60]. We give a brief description of the problem.
 582 Suppose we are given a feature matrix $X \in \mathbb{R}^{n \times d}$ with rows $x_i \in \mathbb{R}^d$. Corresponding-
 583 ly we are given $Y \in \{0, 1\}^n$ the binary response vector for each of the covariates
 584 in our feature matrix. The logistic model for the probability of $y_i = 1$ given $x_i \in \mathbb{R}^d$
 585 and a parameter $\theta \in \mathbb{R}^d$ is

$$586 \quad (4.4) \quad \mathbb{P}(y_i = 1 | x_i, \theta) = \frac{\exp(\theta^T x_i)}{1 + \exp(\theta^T x_i)}.$$

Suppose we impose a prior distribution on the parameter $\theta \sim \mathcal{N}(0, \Sigma_X)$, where
 $\Sigma_X = \frac{1}{n} X^T X$ is the sample covariance of X . Then the posterior distribution for θ
 can be calculated by

$$p(\theta | X, Y) \propto \exp \left[Y^T X \theta - \sum_{i=1}^n \log(1 + \exp(\theta^T x_i)) - \frac{\alpha}{2} \theta^T \Sigma_X \theta \right],$$

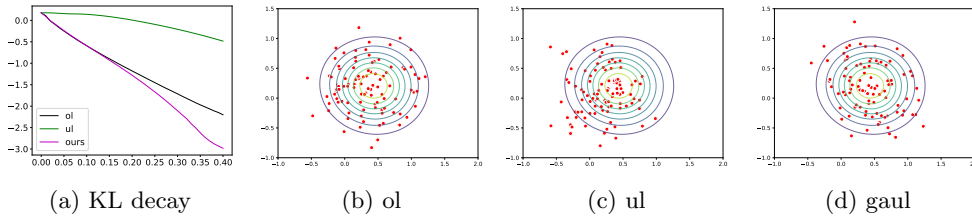


Fig. 7: Convergence and scatter plots for Bayesian logistic regression.

where $\alpha > 0$ is a regularization parameter. The potential function is

$$f(\theta) = -Y^T X \theta + \sum_{i=1}^n \log(1 + \exp(\theta^T x_i)) + \frac{\alpha}{2} \theta^T \Sigma_X \theta.$$

Its gradient is

$$\nabla f(\theta) = -X^T Y + \sum_{i=1}^n \frac{x_i}{1 + \exp(-\theta^T x_i)} + \alpha \Sigma_X \theta.$$

587 As shown in [27], the Hessian of f is upper bounded by $L = (0.25n + \alpha)\lambda_{\max}(\Sigma_X)$ and
 588 lower bounded by $m = \alpha\lambda_{\min}$. To generate X and Y , we set $x_{i,j}$ to be independent
 589 Rademacher random variables for each i and j . And each y_i is generated according
 590 to (4.4) with $\theta = \theta^* = (1, 1)^T$. We set $\alpha = 0.5$, $d = 2$, $n = 50$, $\gamma_{ul} = 2m^{1/2}$
 591 and $\gamma_{pdd} = 2m^{1/2} + m$. To sample the posterior distribution, we use time step
 592 size $h = 10^{-3}$ and run for 400 iterations. The initial distribution of particles is
 593 $\mathcal{N}(0, L^{-1}\mathbf{I})$. As for evaluation metric, we directly evaluate the KL divergence between
 594 the sampled posterior and the true posterior. We use 10^6 particles and $n^2 = 2500$ bins
 595 to evaluate the KL divergence as before. This is different from the choice by [27] and
 596 [60], where [27] compared the samples with θ^* . [60] compared samples with the true
 597 minimizer of $f(\theta)$, i.e. the maximum a posteriori (MAP) estimate in the Bayesian
 598 optimization literature. We believe that directly measuring the KL divergence gives a
 599 better understanding of how ‘close’ our samples are to the true posterior distribution.
 600 The results are presented in Figure 7.

601 **4.6. Bayesian neural network.** In this section, we compare GAUL with over-
 602 damped (‘ol’) and underdamped Langevin (‘ul’) dynamics in training Bayesian neural
 603 network. We test a one-hidden-layer fully connected neural network with 50 hidden
 604 neurons and ReLU activation function on the UCI concrete dataset. We use $h = 10^{-3}$,
 605 $a = 0.1$, $\gamma = 0.5$. For each method, we sample $M = 20$ particles (each particle corre-
 606 sponds to a neural network) and take the average output as the final output. Figure 8a
 607 and Table 1 show the rMSE averaged over 10 experiments. We see that ‘ul’ can achieve
 608 smaller training and validation error than ‘ol’. However, ‘ul’ also exhibits a slow start
 609 and an oscillatory behavior at the beginning of training as is commonly seen in ac-
 610 celeration methods in optimization. GAUL can get rid of the oscillation and achieve
 611 a even smaller training and validation error as is demonstrated in Table 1. We have
 612 also tested out the three methods using the Combined Cycle Power Plant (CCPP)
 613 dataset. We choose the same parameter as the concrete experiment. The results are
 614 presented in Figure 8b and Table 1.

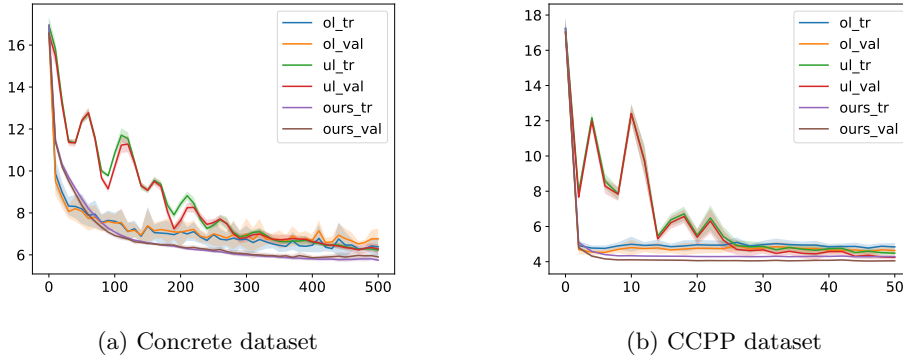


Fig. 8: Convergence comparison. x-axis represents number of epochs. y-axis represents rMSE averaged over 10 experiments.

	ol	ul	gaul
concrete tr err	6.39 ± 0.44	6.23 ± 0.15	5.74 ± 0.06
concrete val err	6.76 ± 0.49	6.28 ± 0.24	5.90 ± 0.14
ccpp tr err	4.84 ± 0.22	4.48 ± 0.11	4.28 ± 0.03
ccpp val err	4.63 ± 0.25	4.25 ± 0.11	4.04 ± 0.04

Table 1: Training and validation rmse.

615 **5. Conclusions.** In this work, we introduced gradient-adjusted underdamped
616 Langevin dynamics (GAUL) inspired by primal-dual damping dynamics and Hessian-
617 driven damping dynamics. We demonstrated that GAUL admitted the correct sta-
618 tionary target distribution $\pi \propto \exp(-f)$ under appropriate conditions and achieves
619 exponential convergence for quadratic functions, outperforming both the overdamped
620 and underdamped Langevin dynamics in terms of convergence speed. Our numerical
621 experiments further illustrate the practical advantages of GAUL, showcasing faster
622 convergence and more efficient sampling compared to classical methods, such as over-
623 damped and underdamped Langevin dynamics.

624 We also note a connection between the primal-dual damping dynamics and GAUL.
625 A key challenge in the primal-dual damping algorithm is the design of preconditioner
626 matrices, which can accelerate the algorithm’s convergence compared to the gradient
627 descent method. In the context of solving a linear problem where f is a quadratic
628 function and the diffusion constant is zero, [67] demonstrates that the convergence
629 rate depends on the square root of the smallest eigenvalue. In this paper, we extend
630 the study from a sampling perspective, where f is also a quadratic function but the
631 diffusion is non-zero. Towards a Gaussian target distribution, GAUL converges to a
632 biased target distribution with the mixing time depending on $\sqrt{\kappa}$. This is in contrast
633 with overdamped and underdamped Langevin sampling algorithms.

634 Several possible future directions are worth exploring. First, can we show that
635 GAUL converges faster than overdamped and underdamped Langevin dynamics for
636 more general potentials, which is beyond the current study of Gaussian distributions?

637 One common assumption is that the potential f is strongly log-concave [8, 17, 18,
638 19, 25, 27, 34, 38, 42]. Recently, [9] proved that for a class of distributions that
639 satisfy a Poincaré-type inequality, underdamped Langevin dynamics converges in L_2
640 with rate $\exp(-\sqrt{m}t)$ where m is the Poincaré constant. Then it is interesting to
641 study for the same class of distributions, whether GAUL could converge at an even
642 faster rate. Another direction is to study the convergence of GAUL under different
643 metrics. From a more practical perspective, designing new time discretization schemes
644 [55, 16, 50, 60, 42] for implementing GAUL is also an important direction. We proved
645 that using the Euler-Maruyama discretization, GAUL will converge to a biased target
646 distribution, which is not surprising since ULA is also biased. Therefore, another
647 promising direction could be to combine GAUL with MCMC methods [7, 27], such as
648 Metropolis-Hastings algorithms, to design a hybrid method with accept/reject options
649 so that the algorithm converges to the correct target distribution in the discrete-
650 time update. Finally, choosing the preconditioner \mathbf{C} to accelerate convergence is an
651 important topic. The difficulty of picking \mathbf{C} arises from the positive semidefinite
652 constraint on $\text{sym}(\mathbf{Q})$ in (2.16), which we should explore in future work.

653 **Appendix A. Euler-Maruyama Discretization.** The Euler-Maruyama
654 scheme of (2.15) with step size h and $\mathbf{C} = \mathbf{I}$ reads

$$655 \quad (\text{A.1a}) \quad \mathbf{x}_{t+1} = \mathbf{x}_t - a\nabla f(\mathbf{x}_t)h + \mathbf{p}_t h + \sqrt{2ah}\mathbf{z}^{(1)},$$

$$656 \quad (\text{A.1b}) \quad \mathbf{p}_{t+1} = \mathbf{p}_t - \nabla f(\mathbf{x}_t)h - \gamma\mathbf{p}_t h + \sqrt{2\gamma h}\mathbf{z}^{(2)}.$$

657 $\mathbf{z}^{(i)}$ is a standard Gaussian random variable for $i = 1, 2$.

658 **Appendix B. A matrix lemma.** Let $a \geq 0$, $s > 0$, $\gamma > 0$, and consider the
659 3×3 matrix

$$660 \quad (\text{B.1}) \quad \mathbf{D} = \begin{pmatrix} -2as & -2\gamma s^{-1} & -s^{-1} \\ 0 & 0 & 1 \\ 2s^2 & 2(-1 - a\gamma)s^{-1} - 2\gamma^2 & -3\gamma - as \end{pmatrix}.$$

661 A direct calculation shows that the eigenvalues are given by

$$662 \quad (\text{B.2a}) \quad \lambda_0(a, \gamma, s) = -as - \gamma,$$

$$663 \quad (\text{B.2b}) \quad \lambda_-(a, \gamma, s) = -as - \gamma - \sqrt{\gamma^2 - 2a\gamma s + s(-4 + a^2 s)},$$

$$664 \quad (\text{B.2c}) \quad \lambda_+(a, \gamma, s) = -as - \gamma + \sqrt{\gamma^2 - 2a\gamma s + s(-4 + a^2 s)}.$$

665 We have the following lemmas regarding the eigenvalues given by (B.2).

LEMMA B.1. *Let \mathbf{D} be as (B.1). If $a = 0$, then*

$$\arg \min_{\gamma > 0} \Re(\lambda_+(0, \gamma, s)) = 2\sqrt{s}.$$

666 *Proof.* We have that $\lambda_+(0, \gamma, s) = \frac{1}{2} \left(-\gamma + \sqrt{\gamma^2 - 4s} \right)$. If $\gamma \leq 2\sqrt{s}$, then $\Re(\lambda_+(0, \gamma, s)) \geq$
667 $-\sqrt{s}$. When $\gamma \geq 2\sqrt{s}$, we have that $\Re(\lambda_+(0, \gamma, s)) = \lambda_+(0, \gamma, s)$. And $\frac{\partial}{\partial \gamma} \lambda_+(0, \gamma, s) \geq$
668 0 . Therefore, the minimum of $\Re(\lambda_+(0, \gamma, s))$ takes place at $\gamma = 2\sqrt{s}$. \square

669 LEMMA B.2. *Let \mathbf{D} be as (B.1). Let $\gamma > 0$ be fixed. Then*

$$670 \quad (\text{B.3}) \quad \arg \min_{a > 0} \Re(\lambda_+(a, \gamma, s)) = \frac{\gamma}{s} + \frac{2}{\sqrt{s}}.$$

Proof. Let us define $\Delta(a) = \gamma^2 - 2a\gamma s + s(a^2s - 4)$. It can be seen that Δ is a quadratic function of a . The two roots of Δ are given by

$$a_{\pm} = \frac{\gamma}{s} \pm \frac{2}{\sqrt{s}}.$$

When $a \in [a_-, a_+]$, $\Delta(a) \leq 0$ and

$$\Re(\lambda_+(a, \gamma, s)) = \frac{1}{2}(-\gamma - as) \geq \frac{1}{2}(-\gamma - a_+s) = \Re(\lambda_+(a_+, \gamma, s)) = -\gamma - \sqrt{s}.$$

When $a < a_-$, we can calculate that

$$\frac{\partial}{\partial a} \lambda_+(a, \gamma, s) = -s + \frac{-\gamma s + as^2}{\sqrt{\Delta}} < 0.$$

671 This implies that $\lambda_+(a_- - \varepsilon, \gamma, s) > \lambda_+(a_-, \gamma, s)$ for any $\varepsilon > 0$. Similarly, when
672 $a > a_+$, we have that $\frac{\partial}{\partial a} \lambda_+(a, \gamma, s) > 0$. Thus, $\lambda_+(a_+ + \varepsilon, \gamma, s) > \lambda_+(a_+, \gamma, s)$ for any
673 $\varepsilon > 0$. Combining the above results, we conclude our proof. \square

674 **LEMMA B.3.** *Let \mathbf{D} be as (B.1). Let $a > 0$ be fixed. Then*

$$675 \text{ (B.4)} \quad \arg \min_{\gamma > 0} \Re(\lambda_+(a, \gamma, s)) = as + 2\sqrt{s}.$$

Proof. The proof will be similar to that of Lemma B.2. This time we define $\Delta(\gamma) = \gamma^2 - 2a\gamma s + s(a^2s - 4)$. It can be seen that $\Delta(\gamma)$ is a quadratic function of γ . The two roots of $\Delta(\gamma)$ are given by

$$\gamma_{\pm} = as \pm 2\sqrt{s}.$$

When $\gamma \in [\gamma_-, \gamma_+]$, $\Delta(\gamma) < 0$ and

$$\Re(\lambda_+(a, \gamma, s)) = \frac{1}{2}(-\gamma - as) \geq \frac{1}{2}(-\gamma_+ - as) = \Re(\lambda_+(a, \gamma_+, s)) = -as - \sqrt{s}.$$

676 When $\gamma < \gamma_-$, we have

$$677 \quad \frac{\partial}{\partial \gamma} \lambda_+(a, \gamma, s) = -1 + \frac{\gamma - as}{\sqrt{(\gamma - as)^2 - 4s}}$$

$$678 \quad \leq -1 < 0,$$

679 since $\gamma - as < 0$. When $\gamma > \gamma_+$, we have

$$680 \quad \frac{\partial}{\partial \gamma} \lambda_+(a, \gamma, s) = -1 + \frac{\gamma - as}{\sqrt{(\gamma - as)^2 - 4s}}$$

$$681 \quad \geq -1 + 1 = 0.$$

682 Combining the above arguments, we conclude that the optimal γ is γ_+ . \square

683 We now turn to a more general setting. Let $a \geq 0$, $\gamma > 0$ and define

$$684 \text{ (B.5)} \quad \mathcal{D} = \begin{pmatrix} -2a\mathbf{S} & -2\gamma\mathbf{S}^{-1} & -\mathbf{S}^{-1} \\ 0 & 0 & \mathbf{I} \\ 2\mathbf{S}^2 & 2(-1 - a\gamma)\mathbf{S}^{-1} - 2\gamma^2\mathbf{I} & -3\gamma\mathbf{I} - a\mathbf{S} \end{pmatrix},$$

685 where now \mathbf{S} is a diagonal matrix whose diagonal is given by $s_1 \geq s_2 \geq \dots \geq s_d > 0$.
686 And \mathbf{I} is the identity matrix. Just like Lemma B.1, Lemma B.2, and Lemma B.7 we
687 want to characterize the eigenvalues of \mathcal{D} . In particular, we would like to characterize
688 the largest real part of the eigenvalue of \mathcal{D} in terms of a and γ .

689 PROPOSITION B.4. *The eigenvalues for \mathcal{D} are given by*

690 (B.6a) $\lambda_0^{(i)}(a, \gamma, \mathbf{S}) = -as_i - \gamma,$

691 (B.6b) $\lambda_-^{(i)}(a, \gamma, \mathbf{S}) = -as_i - \gamma - \sqrt{\gamma^2 - 2a\gamma s_i + s_i(-4 + a^2 s_i)},$

692 (B.6c) $\lambda_+^{(i)}(a, \gamma, \mathbf{S}) = -as_i - \gamma + \sqrt{\gamma^2 - 2a\gamma s_i + s_i(-4 + a^2 s_i)},$

693 *for $i = 1, \dots, d$. The corresponding eigenvectors are sparse and take the following*
 694 *form. (Here we only write out the non-zero part of the eigenvectors)*

695 (B.7a) $v_{0,i}^{(i)} = \frac{-1}{s_i(\gamma + as_i)},$

696 (B.7b) $v_{0,i+d}^{(i)} = \frac{-1}{\gamma + as_i},$

697 (B.7c) $v_{0,i+2d}^{(i)} = 1,$

698

699 (B.8a) $v_{-,i}^{(i)} = \frac{2\gamma - \sqrt{\gamma^2 - 2a\gamma s_i + s_i(a^2 s_i - 4)} - \frac{2(\gamma^2 + s_i + a\gamma s_i)}{\gamma + as_i + \sqrt{\gamma^2 - 2a\gamma s_i + s_i(a^2 s_i - 4)}}}{2s_i^2},$

700 (B.8b) $v_{-,i+d}^{(i)} = \frac{-1}{\gamma + as_i + \sqrt{\gamma^2 - 2a\gamma s_i + s_i(a^2 s_i - 4)}},$

701 (B.8c) $v_{-,i+2d}^{(i)} = 1,$

702

703 (B.9a) $v_{+,i}^{(i)} = \frac{2\gamma + \sqrt{\gamma^2 - 2a\gamma s_i + s_i(a^2 s_i - 4)} - \frac{2(\gamma^2 + s_i + a\gamma s_i)}{\gamma + as_i - \sqrt{\gamma^2 - 2a\gamma s_i + s_i(a^2 s_i - 4)}}}{2s_i^2},$

704 (B.9b) $v_{+,i+d}^{(i)} = \frac{-1}{\gamma + as_i - \sqrt{\gamma^2 - 2a\gamma s_i + s_i(a^2 s_i - 4)}},$

705 (B.9c) $v_{+,i+2d}^{(i)} = 1.$

706 *In the above, $v_{*,j}^{(i)}$ represents the j -th component of the eigenvector corresponding to*
 707 *the eigenvalue $\lambda_*^{(i)}$, where $*$ \in $\{0, +, -\}$.*

708 *Moreover, when γ is chosen according to Lemma B.7, we have a defective eigen-*
 709 *value $\lambda_0^{(d)} = \lambda_{\pm}^{(d)} = -as_d - \gamma$, which is accompanied with two generalized eigenvectors*
 710 *η, ξ that satisfy $(\mathcal{D} - \lambda_0^{(d)})\eta = v_0^{(d)}$, $(\mathcal{D} - \lambda_0^{(d)})\xi = v_0^{(d)}$. In details, the nonzero*
 711 *components of $v_0^{(d)}$, η and ξ are given by*

712 (B.10a) $v_{0,d}^{(d)} = \frac{-1}{s_d(\gamma + as_d)},$

713 (B.10b) $v_{0,2d}^{(d)} = \frac{-1}{\gamma + as_d},$

714 (B.10c) $v_{0,3d}^{(d)} = 1,$

715

716 (B.11a) $\eta_d = \frac{\gamma - as}{2s_d^2},$

717 (B.11b) $\eta_{3d} = 1,$

718

$$719 \quad (\text{B.12a}) \quad \xi_d = \frac{\gamma^2 - (1 + a\gamma)s_d}{s_d^2},$$

$$720 \quad (\text{B.12b}) \quad \xi_{2d} = 1.$$

721 *Proof.* One can directly verify that the above computation gives an eigensystem
722 for \mathcal{D} . \square

723 From the sparsity structure of $v_{\pm}^{(j)}$ and $v_0^{(j)}$, we immediately have the following corol-
724 lary.

725 **COROLLARY B.5.** $v_{\star}^{(j)}$ is orthogonal to $v_{\star}^{(k)}$ for $\star, \star \in \{0, +, -\}$ if $j \neq k$.

726 **LEMMA B.6.** Let \mathcal{D} be as (B.5). If $a = 0$, then

$$727 \quad (\text{B.13}) \quad \arg \min_{\gamma > 0} \max_j \Re(\lambda_+^{(j)}(0, \gamma, \mathbf{S})) = 2\sqrt{s_d}.$$

Proof. Plugging $a = 0$ into (B.6) we have

$$\lambda_+^{(j)}(0, \gamma, \mathbf{S}) = \frac{1}{2} \left(-\gamma + \sqrt{\gamma^2 - 4s_j} \right).$$

We first note that since $s_d \leq s_{d-1} \leq \dots \leq s_1$, if $\gamma \leq 2\sqrt{s_d}$ then $\Re(\lambda_+^{(j)}(0, \gamma, \mathbf{S})) = -\gamma/2$ for all $1 \leq j \leq d$. In particular, this implies that

$$\arg \min_{0 < \gamma \leq 2\sqrt{s_d}} \max_j \Re(\lambda_+^{(j)}(0, \gamma, \mathbf{S})) = 2\sqrt{s_d}.$$

We then need to show that if $\gamma > 2\sqrt{s_d}$, $\max_j \Re(\lambda_+^{(j)}(0, \gamma, \mathbf{S})) > -\sqrt{s_d}$. This will be very similar to the argument in the proof of Lemma B.1. Now consider $\gamma > 2\sqrt{s_d}$. We showed in the proof of Lemma B.1 that $\Re(\lambda_+^{(n)}(0, \gamma, \mathbf{S})) = \lambda_+^{(n)}(0, \gamma, \mathbf{S})$. And $\frac{\partial}{\partial \gamma} \lambda_+^{(n)}(0, \gamma, \mathbf{S}) \geq 0$. Hence, we have

$$\max_j \Re(\lambda_+^{(j)}(0, \gamma, \mathbf{S})) > \Re(\lambda_+^{(n)}(0, \gamma, \mathbf{S})) = \lambda_+^{(n)}(0, \gamma, \mathbf{S}) \geq \lambda_+^{(n)}(0, 2\sqrt{s_d}, \mathbf{S}) = -\sqrt{s_d}.$$

728 This concludes our proof. \square

729 **LEMMA B.7.** Let \mathcal{D} be as (B.5). Let $a > 0$. Then

$$730 \quad (\text{B.14}) \quad \arg \min_{\gamma > 0} \max_j \Re(\lambda_+^{(j)}(a, \gamma, \mathbf{S})) = as_d + 2\sqrt{s_d}.$$

Proof. Let us define $\Delta(\gamma, s) = \gamma^2 - 2a\gamma s + s(a^2 s - 4)$. A straightforward calculation shows that the two roots of $\Delta(\gamma, s_j)$ (when viewing Δ as a function of γ) are given by

$$\gamma_{\pm}^{(j)} = as_j \pm 2\sqrt{s_j}.$$

We have shown in Lemma B.3 that

$$\arg \min_{\gamma > 0} \Re(\lambda_+^{(d)}(a, \gamma, \mathbf{S})) = as_d + 2\sqrt{s_d}.$$

731 Denote by $\gamma^*(a) = as_d + 2\sqrt{s_d}$. Let us consider $\tilde{s} > s_d$. If $\Delta(\gamma^*(a), \tilde{s}) \leq 0$, then we
 732 have

$$\begin{aligned}
 733 \quad \Re\left(-\gamma^*(a) - a\tilde{s} + \sqrt{\gamma^*(a)^2 - 2a\gamma^*(a)\tilde{s} + \tilde{s}(a^2\tilde{s} - 4)}\right) &= -\gamma^*(a) - a\tilde{s} \\
 734 &\leq -\gamma^*(a) - as_d \\
 735 \quad (\text{B.15}) &= \Re(\lambda_+^{(d)}(a, \gamma^*(a), \mathbf{S})),
 \end{aligned}$$

736 where the last line follows from $\Delta(\gamma^*(a), s_d) = 0$ by definition of $\gamma^*(a)$. If $\Delta(\gamma^*(a), \tilde{s}) > 0$,
 737 we compute

$$\begin{aligned}
 738 \quad \frac{\partial}{\partial \tilde{s}} \left(-\gamma^*(a) - as + \sqrt{\gamma^*(a)^2 - 2a\gamma^*(a)s + s(a^2s - 4)} \right) \Big|_{s=\tilde{s}} \\
 739 \quad (\text{B.16}) \quad = -a + \frac{-a\gamma^*(a) + a^2\tilde{s} - 2}{\sqrt{\gamma^*(a)^2 - 2a\gamma^*(a)\tilde{s} + \tilde{s}(a^2\tilde{s} - 4)}} > 0.
 \end{aligned}$$

We now verify that the above derivative is indeed positive. First observe that given $\tilde{s} > s_d$, the two roots for $\Delta(\gamma, \tilde{s})$ are

$$\tilde{\gamma}_{\pm} = a\tilde{s} \pm 2\sqrt{\tilde{s}}.$$

740 Clearly, $\tilde{\gamma}_+ > \gamma^*(a)$. Hence, $\Delta(\gamma^*(a), \tilde{s}) > 0$ implies that $\gamma^*(a) < \tilde{\gamma}_-$, or equivalently
 741 $\tilde{s} > s_d + (2\sqrt{s_d} + 2\sqrt{\tilde{s}})/a$. This further implies $\sqrt{\tilde{s}} > 2/a$. Therefore,

$$\begin{aligned}
 742 \quad -a\gamma^*(a) + a^2\tilde{s} - 2 &> a^2(s_d + (2\sqrt{s_d} + 2\sqrt{\tilde{s}})/a) - a\gamma^*(a) - 2 \\
 743 &= 2a\sqrt{\tilde{s}} - 2 \\
 744 &> 2a\frac{2}{a} - 2 > 0.
 \end{aligned}$$

Knowing that the numerator in the second term of (B.16) is positive, we know that (B.16) is positive if and only if

$$(-a\gamma^*(a) + a^2\tilde{s} - 2)^2 > a^2(\gamma^*(a)^2 - 2a\gamma^*(a)\tilde{s} + \tilde{s}(a^2\tilde{s} - 4)),$$

745 which can be verified by expanding the square on the left hand side and comparing
 746 with the right hand side directly.

747 Since the derivative in (B.16) is positive, let us examine the limit

$$\begin{aligned}
 748 \quad \lim_{s \rightarrow \infty} -\gamma^*(a) - as + \sqrt{\gamma^*(a)^2 - 2a\gamma^*(a)s + s(a^2s - 4)} \\
 749 \quad = \lim_{s \rightarrow \infty} -\gamma^*(a) - as + s\sqrt{\gamma^*(a)^2s^{-2} - 2a\gamma^*(a)s^{-1} + a^2 - 4s^{-1}} \\
 750 \quad = \lim_{s \rightarrow \infty} -\gamma^*(a) - as + as - \left(\gamma^*(a) + \frac{2}{a}\right) + \mathcal{O}(s^{-1}) \\
 751 \quad = -2\gamma^*(a) - \frac{2}{a} \\
 752 \quad (\text{B.17}) \quad = -2(as_d + 2\sqrt{s_d}) - \frac{2}{a} < \Re(\lambda_+^{(d)}(a, \gamma^*(a), \mathbf{S})). \quad \square
 \end{aligned}$$

Combining (B.15), (B.16) and (B.17), we obtain that for $1 \leq j \leq d$

$$\Re(\lambda_+^{(j)}(a, \gamma^*(a), \mathbf{S})) \leq \lambda_+^{(d)}(a, \gamma^*(a), \mathbf{S}) = \Re(\lambda_+^{(d)}(a, \gamma^*(a), \mathbf{S})),$$

which implies

$$\min_{\gamma > 0} \max_j \Re(\lambda_+^{(j)}(a, \gamma, \mathbf{S})) \leq \max_j \Re(\lambda_+^{(j)}(a, \gamma^*(a), \mathbf{S})) = \Re(\lambda_+^{(d)}(a, \gamma^*(a), \mathbf{S})).$$

Finally, by Lemma B.3 again, we have

$$\min_{\gamma > 0} \max_j \Re(\lambda_+^{(j)}(a, \gamma, \mathbf{S})) \geq \min_{\gamma > 0} \Re(\lambda_+^{(d)}(a, \gamma, \mathbf{S})) = \Re(\lambda_+^{(d)}(a, \gamma^*(a), \mathbf{S})).$$

We now conclude that

$$\arg \min_{\gamma > 0} \max_j \Re(\lambda_+^{(j)}(a, \gamma, \mathbf{S})) = \gamma^*(a).$$

753 LEMMA B.8. *The constant C_1 in Equation (3.9) depends at most polynomially on*
754 *$d, s_1, 1/s_d$, i.e. $C_1 = \text{poly}(d, s_1, s_d^{-1}) \leq \text{poly}(d, \kappa)$.*

Proof. First, we show that C_1 depends linearly on the dimension d . Let us recall the following fact from linear ODE: if $\dot{x} = Ax$ for some constant matrix $A \in \mathbb{R}^{d \times d}$, with eigenvalues $\lambda_1, \dots, \lambda_d$ and eigenvectors v_1, \dots, v_d , then the solution is of the form $x(t) = \sum_i a_i e^{\lambda_i t} v_i$. In case there are repeated eigenvalues (e.g. λ_i) and generalized eigenvectors, the corresponding term in the sum will be replaced with some $\sum_j b_j t^{k-j} e^{\lambda_i t} v_i$ where the sum is over $j = 1, \dots, k$ and k is the dimension of the generalized eigenspace associated with λ_i . Let \mathcal{D} and \mathbf{T} be as defined in (3.8). By our choice of γ , we know that eigenvalues of \mathcal{D} are nonzero. Therefore, \mathcal{D} is invertible. Denote by

$$\mathbf{Y}(t) = \begin{pmatrix} \Sigma_{11}(t) \\ \Sigma_{22}(t) \\ \dot{\Sigma}_{22}(t) \end{pmatrix} + \mathcal{D}^{-1} \mathbf{T}.$$

755 Then (3.8) reads

$$756 \quad (\text{B.18}) \quad \frac{d}{dt} \mathbf{Y} = \mathcal{D} \mathbf{Y}.$$

757 We follow the notation in Proposition B.4 and use $(\lambda_*^{(i)}, v_*^{(i)})$ to represent an eigenvalue
758 eigenvector pair of \mathcal{D} , for $i = 1, \dots, d$, and $*$ $\in \{0, +, -\}$. Note that for our choice
759 of $\gamma = as_d + 2\sqrt{s_d}$, we have $\lambda_0^{(d)} = \lambda_{\pm}^{(d)}$. Correspondingly, there will be generalized
760 eigenvectors. Following the notation in Proposition B.4, we use $v_0^{(d)}$ to represent the
761 eigenvector associated with $\lambda_0^{(d)}$; and we use η and ξ to represent the generalized
762 eigenvectors associated with $\lambda_0^{(d)}$. We have already shown in Proposition B.4 that
763 both η and ξ are generalized eigenvector of rank 2. Therefore, the solution to (B.18)
764 takes the form

$$765 \quad \mathbf{Y}(t) = \left(\sum_{i=1}^{d-1} \sum_{* \in \{0, +, -\}} \alpha_*^{(i)} e^{\lambda_*^{(i)} t} v_*^{(i)} \right) + \alpha_0^{(d)} e^{\lambda_0^{(d)} t} v_0^{(d)} + \alpha_-^{(d)} e^{\lambda_0^{(d)} t} (t v_0^{(d)} + \eta)$$

$$766 \quad (\text{B.19}) \quad + \alpha_+^{(d)} e^{\lambda_0^{(d)} t} (t v_0^{(d)} + \xi),$$

where the constants $\alpha_*^{(i)}$ are to be determined by $\mathbf{Y}(0)$. By Lemma B.7 and our choice of γ , we have that

$$\max_{i \leq d} \max_{* \in \{0, +, -\}} \Re(\lambda_*^{(i)}) = \lambda_0^{(d)} = -2as_d - 2\sqrt{s_d}.$$

767 Without loss of generality, consider $t \geq 1$. We have

$$\begin{aligned}
768 \quad \|\mathbf{Y}(t)\|^2 &= \left\| \left(\sum_{i=1}^{d-1} \sum_{* \in \{0,+, -\}} \alpha_*^{(i)} e^{\lambda_*^{(i)} t} v_*^{(i)} \right) + \alpha_0^{(d)} e^{\lambda_0^{(d)} t} v_0^{(d)} + \alpha_-^{(d)} e^{\lambda_-^{(d)} t} (tv_0^{(d)} + \eta) \right. \\
769 \quad &\quad \left. + \alpha_+^{(d)} e^{\lambda_+^{(d)} t} (tv_0^{(d)} + \xi) \right\|^2 \\
770 \quad &= \sum_{i=1}^{d-1} \left\| \sum_{* \in \{0,+, -\}} \alpha_*^{(i)} e^{\lambda_*^{(i)} t} v_*^{(i)} \right\|^2 + \left\| \alpha_0^{(d)} e^{\lambda_0^{(d)} t} v_0^{(d)} + \alpha_-^{(d)} e^{\lambda_-^{(d)} t} (tv_0^{(d)} + \eta) \right. \\
771 \quad &\quad \left. + \alpha_+^{(d)} e^{\lambda_+^{(d)} t} (tv_0^{(d)} + \xi) \right\|^2 \\
772 \quad &\leq \sum_{i=1}^{d-1} \sum_{* \in \{0,+, -\}} 3 \left\| \alpha_*^{(i)} e^{\lambda_*^{(i)} t} v_*^{(i)} \right\|^2 + 3 \left\| \alpha_0^{(d)} e^{\lambda_0^{(d)} t} v_0^{(d)} \right\|^2 + 3 \left\| \alpha_-^{(d)} e^{\lambda_-^{(d)} t} (tv_0^{(d)} + \eta) \right\|^2 \\
773 \quad &\quad + 3 \left\| \alpha_+^{(d)} e^{\lambda_+^{(d)} t} (tv_0^{(d)} + \xi) \right\|^2 \\
774 \quad &\leq 3t^2 e^{2\lambda_0^{(d)} t} \left[\left(\sum_{i=1}^{d-1} \sum_{* \in \{0,+, -\}} \left\| \alpha_*^{(i)} v_*^{(i)} \right\|^2 \right) + \left\| v_0^{(d)} \right\|^2 \left((\alpha_0^{(d)})^2 + 2(\alpha_-^{(d)})^2 + 2(\alpha_+^{(d)})^2 \right) \right. \\
775 \quad &\quad \left. + 2 \|\eta\|^2 (\alpha_-^{(d)})^2 + 2 \|\xi\|^2 (\alpha_+^{(d)})^2 \right] \\
776 \quad &\leq 6t^2 e^{2\lambda_0^{(d)} t} \left[\left(\sum_{i=1}^{d-1} \sum_{* \in \{0,+, -\}} \left\| \alpha_*^{(i)} v_*^{(i)} \right\|^2 \right) + \left\| v_0^{(d)} \right\|^2 \left((\alpha_0^{(d)})^2 + (\alpha_-^{(d)})^2 + (\alpha_+^{(d)})^2 \right) \right. \\
777 \quad &\quad \left. + \|\eta\|^2 (\alpha_-^{(d)})^2 + \|\xi\|^2 (\alpha_+^{(d)})^2 \right] \\
778 \quad &\leq 6t^2 e^{2\lambda_0^{(d)} t} \left[\left(\sum_{i=1}^{d-1} \sum_{* \in \{0,+, -\}} \left\| \alpha_*^{(i)} v_*^{(i)} \right\|^2 \right) + \left(\left\| \alpha_+^{(d)} v_0^{(d)} \right\|^2 + \left\| \alpha_-^{(d)} \eta \right\|^2 + \left\| \alpha_+^{(d)} \xi \right\|^2 \right) \right. \\
779 \quad &\quad \left. \left(1 + \frac{\left\| v_0^{(d)} \right\|^2}{\|\xi\|^2} + \frac{\left\| v_0^{(d)} \right\|^2}{\|\eta\|^2} \right) \right] \\
780 \quad &\leq 6t^2 e^{2\lambda_0^{(d)} t} \left(1 + \frac{\left\| v_0^{(d)} \right\|^2}{\|\xi\|^2} + \frac{\left\| v_0^{(d)} \right\|^2}{\|\eta\|^2} \right) \left[\sum_{i=1}^{d-1} \sum_{* \in \{0,+, -\}} \left\| \alpha_*^{(i)} v_*^{(i)} \right\|^2 \right. \\
(B.20) \quad &\quad \left. + \left\| \alpha_+^{(d)} v_0^{(d)} \right\|^2 + \left\| \alpha_-^{(d)} \eta \right\|^2 + \left\| \alpha_+^{(d)} \xi \right\|^2 \right]. \quad \square
\end{aligned}$$

$$\|\mathbf{Y}(0)\|^2 = \sum_{i=1}^{d-1} \left\| \sum_{* \in \{0,+, -\}} \alpha_*^{(i)} v_*^{(i)} \right\|^2 + \left\| \alpha_0^{(d)} v_0^{(d)} + \alpha_-^{(d)} \eta + \alpha_+^{(d)} \xi \right\|^2.$$

Denote by $\mathbf{Y}(0)^{(i)}$ the projection of $\mathbf{Y}(0)$ onto the subspace $\Phi_i = \text{Span}(\{v_0^{(i)}, v_+^{(i)}, v_-^{(i)}\})$. And accordingly, $\Phi_d = \text{Span}(\{v_0^{(d)}, \eta, \xi\})$. By Corollary B.5, we know that Φ_i is orthogonal to Φ_j for $i \neq j$. Therefore, $|\alpha_*^{(i)}|$ depends on the inverse of the Gram matrix of $\{v_0^{(i)}, v_+^{(i)}, v_-^{(i)}\}$ as well as $\|\mathbf{Y}(0)^{(i)}\|$. This inverse Gram matrix can be computed analytically since it is a 3 by 3 matrix for each $1 \leq i \leq d$. However, the exact computation does not add more insights to the proof and we will not include the computation. Since each eigenvector and generalized eigenvector depends on $\{s_1, \dots, s_d, s_1^{-1}, \dots, s_d^{-1}\}$ polynomially, we know that the inverse of the Gram matrix also depends on $\{s_1, \dots, s_d, s_1^{-1}, \dots, s_d^{-1}\}$ polynomially. From (B.20), we conclude that

$$\|\mathbf{Y}(t)\|^2 = \mathcal{O}(t^2 e^{2\lambda_0^{(d)} t} d^2 \cdot \text{poly}(s_1, s_d^{-1})) = \mathcal{O}(t^2 e^{2\lambda_0^{(d)} t} d^2 \cdot \text{poly}(\kappa)).$$

LEMMA B.9. Suppose $X \in \mathbb{S}^n$ satisfies $X = AXA^T$ for some $A \in \mathbb{R}^n$. If all eigenvalues of A has absolute value less than 1, then X is the zero matrix.

Proof. Let us first assume that A^T is diagonalizable: $A^T = QDQ^{-1}$, where D is a diagonal matrix of eigenvalues d_1, \dots, d_n , and the columns of Q contains the eigenvectors q_1, \dots, q_n . Then it follows that

$$|q_i^T X q_j| = |d_i d_j| |q_i^T X q_j|.$$

This implies $|q_i^T X q_j| = 0$ for all $1 \leq i, j \leq n$, since $|d_i d_j| < 1$ by assumption. Now suppose that A has some generalized eigenvalues. Without loss of generality, assume that d_{n-1} is a generalized eigenvalue such that $A^T q_{n-1} = d_{n-1} q_{n-1}$ and $A^T q_n = d_{n-1} q_n + q_{n-1}$. Let q_i be an eigenvector. Then we still have $q_i^T X q_{n-1} = 0$ as before. And

$$|q_i^T X q_n| = |d_i d_{n-1} q_i^T X q_n + d_i q_i^T X q_{n-1}| = |d_i d_{n-1} q_i^T X q_n| = |d_i d_{n-1}| |q_i^T X q_n|.$$

Again this implies $|q_i^T X q_n| = 0$. The case where d_{n-1} has algebraic multiplicity greater than 2 or q_i is a generalized eigenvector can be proved in a similar fashion. Therefore, we have shown that if A has Jordan decomposition $A = PJP^{-1}$, then $q_i^T X q_j = 0$ where q_i and q_j are the i -th and j -th column of P . Equivalently, we have $P^T X P = 0$. This proves that $X = 0$. \square

COROLLARY B.10. Suppose $X, Y \in \mathbb{S}^n$ satisfy $X = AXA^T + B$, $Y = AY A^T + B$ for some $B \in \mathbb{S}^n$. If all eigenvalues of A have absolute value less than 1, then $X = Y$.

Proof. The proof follows by Lemma B.9 and that $X - Y = A(X - Y)A^T$. \square

Taking inspiration from system of linear ODE, we have the following lemma regarding the solution to the iteration $X_{k+1} = AX_k A^T$.

LEMMA B.11. Let $A \in \mathbb{R}^{n \times n}$ be given by $A = \mathbf{I} - h\tilde{G}$ for some $\tilde{G} \in \mathbb{R}^{n \times n}$, $h > 0$. Suppose \tilde{G} has Jordan decomposition $\tilde{G} = PJP^{-1}$. And consider the iteration $X_{k+1} = AX_k A^T$. If q_i is an eigenvector of \tilde{G} with associated eigenvalue d_i and $X_0 = q_i q_i^T$, then $X_k = (1 - hd_i)^{2k} X_0$. Moreover, if q_i is a generalized eigenvector of \tilde{G} of algebraic multiplicity 2, i.e. $\tilde{G} q_i = d_j q_i + q_j$ for some eigenvector q_j and eigenvalue d_j , and $X_0 = q_i q_i^T$, then $X_k = ((1 - hd_j)^k q_i - kh(1 - hd_j)^{k-1} q_j)((1 - hd_j)^k q_i - kh(1 - hd_j)^{k-1} q_j)^T$.

LEMMA B.12. The eigenvalues of \mathbf{G} in (3.11) are given by the following

$$(B.21) \quad \tilde{\lambda}_{\pm}^{(i)} = h \frac{(as_i + \gamma) \pm \sqrt{(as_i - \gamma)^2 - 4s_i}}{2}.$$

803 *Proof.* The proof follows by a direct computation. \square

804 LEMMA B.13. Consider $\gamma = \gamma^* = as_d + 2\sqrt{s_d}$. Let $s > s_d$. Then $a \leq \frac{2}{\sqrt{s} - \sqrt{s_d}}$ if
805 and only if $(as - \gamma^*)^2 - 4s \leq 0$.

Proof. Multiplying by $s - s_d$, we obtain

$$a \leq \frac{2}{\sqrt{s} - \sqrt{s_d}} \iff a(s - s_d) \leq 2\sqrt{s} + 2\sqrt{s_d} \iff as - 2\sqrt{s} \leq \gamma^*.$$

806 And it is straightforward to verify that $2\sqrt{s} > -as + \gamma^*$ always holds. Squaring on
807 both hand sides completes the proof. \square

LEMMA B.14. Consider $\tilde{\lambda}_{\pm}^{(i)}$ given by (B.21). Suppose $a \geq \frac{2}{\sqrt{s_1} - \sqrt{s_d}}$. If the step
size h satisfies $0 < h \leq 1/(as_1 + \gamma)$, and $\gamma = \gamma^* = as_d + 2\sqrt{s_d}$, then

$$\max_i |1 - \tilde{\lambda}_{\pm}^{(i)}| \leq 1 - \frac{h}{2}(as_d + \sqrt{s_d}).$$

Proof. Observe that the eigenvalues given in (B.21) is almost the same as the
eigenvalues given in (B.6) except for an extra factor of $h/2$. This allows us to use
previous lemma regarding the eigenvalues from (B.6). We consider two cases. Define

$$j = \inf \left\{ n : a \leq \frac{2}{\sqrt{s_n} - \sqrt{s_d}} \right\}.$$

808 **Case 1:** Consider $i \leq j-1$ (if $j = 1$, we directly consider Case 2). Then $a \geq \frac{2}{\sqrt{s_i} - \sqrt{s_d}}$.
809 By Lemma B.13 and our assumption on a , we have $(as_i - \gamma^*)^2 - 4s_i \geq 0$. Then, one
810 can verify that $0 < h \leq \frac{1}{as_1 + \gamma^*}$ is a sufficient condition for $1 - \tilde{\lambda}_{\pm}^{(i)} > 0$. Indeed, we
811 compute

$$\begin{aligned} 812 \quad \tilde{\lambda}_{\pm}^{(i)} &\leq \frac{1}{as_1 + \gamma^*} \frac{(as_i + \gamma^*) + \sqrt{(as_i - \gamma^*)^2 - 4s_i}}{2} \\ 813 &\leq \frac{1}{as_1 + \gamma^*} \frac{(as_i + \gamma^*) + \sqrt{(as_i + \gamma^*)^2}}{2} \\ 814 &= \frac{as_i + \gamma^*}{as_1 + \gamma^*} \\ 815 \quad (\text{B.22}) &\leq 1. \end{aligned}$$

816 Moreover, we clearly have $\tilde{\lambda}_{\pm}^{(i)} > 0$. Therefore, $|1 - \tilde{\lambda}_{\pm}^{(i)}| \leq 1$. On the other hand, by
817 (B.16) and (B.17), we have that

$$\begin{aligned} 818 \quad \tilde{\lambda}_{\pm}^{(i)} &\geq \lim_{s \rightarrow \infty} \frac{h}{2} \left((as + \gamma^*) + \sqrt{(as - \gamma^*)^2 - 4s} \right) \\ 819 &= \frac{h}{2} \left(2\gamma^* + \frac{2}{a} \right) \\ 820 &\geq h\gamma^*. \end{aligned}$$

Therefore,

$$\max_{i \leq j-1} |1 - \tilde{\lambda}_{\pm}^{(i)}| \leq 1 - h(as_d + 2\sqrt{s_d}).$$

Case 2: Consider $i \geq j$. Note that for a complex number $z = z_1 + iz_2$ and $h > 0$, we have that

$$|1 - hz|^2 = (1 - hz_1)^2 + h^2 z_2^2 \leq 1 - hz_1 \leq (1 - hz_1/2)^2,$$

821 where the first inequality holds if and only if $h \leq z_1/(z_1^2 + z_2^2)$. Therefore, we have

$$822 \quad |1 - \tilde{\lambda}_{\pm}^{(i)}|^2 \leq \left(1 - \frac{\Re(\tilde{\lambda}_{\pm}^{(i)})}{2}\right)^2,$$

if

$$h \leq \frac{2(as_i + \gamma^*)}{(as_i + \gamma^*)^2 + 4s_i - (as_i - \gamma^*)^2} = \frac{as_i + \gamma^*}{2as_i\gamma^* + 2s_i}.$$

We now verify that $h \leq 1/(as_1 + \gamma^*)$ is a sufficient condition. We have

$$\frac{1}{as_1 + \gamma^*} \leq \frac{as_i + \gamma^*}{2as_i\gamma^* + 2s_i} \iff a^2s_1s_i + \gamma^*as_1 + (\gamma^*)^2 \geq as_i\gamma^* + 2s_i.$$

823 By Lemma B.13, we have that

$$824 \quad a^2s_1^2 + (\gamma^*)^2 - 2as_1\gamma^* \geq 4s_1$$

$$825 \quad a^2s_1 + \frac{(\gamma^*)^2}{s_1} - 2a\gamma^* \geq 4$$

$$826 \quad a^2s_1 \geq 4 + 2a\gamma^* - \frac{(\gamma^*)^2}{s_1}.$$

827 Then

$$\begin{aligned} 828 \quad a^2s_1s_i + \gamma^*as_1 + (\gamma^*)^2 &\geq s_i\left(4 + 2a\gamma^* - \frac{(\gamma^*)^2}{s_1}\right) + \gamma^*as_1 + (\gamma^*)^2 \\ 829 \quad &= 4s_i + 2a\gamma^*s_i - \frac{s_i(\gamma^*)^2}{s_1} + \gamma^*as_1 + (\gamma^*)^2 \\ 830 \quad &\geq 4s_i + 2a\gamma^*s_i + \gamma^*as_1 \\ 831 \quad &> as_i\gamma^* + 2s_i. \end{aligned}$$

This shows that $h \leq 1/(as_1 + \gamma^*)$ is sufficient. By Lemma B.7 and our choice of h , we obtain that

$$\max_{i \geq j} |1 - \tilde{\lambda}_{\pm}^{(i)}| < \max_i 1 - \frac{\Re(\tilde{\lambda}_{\pm}^{(i)})}{2} \leq 1 - \frac{h}{2}(as_d + \sqrt{s_d}).$$

832 Combining the two cases, we complete the proof. \square

LEMMA B.15. Consider $\tilde{\lambda}_{\pm}^{(i)}$ given by (B.21). Suppose $a = 0$ and $\gamma = \gamma^* = 2\sqrt{s_d}$. Then

$$\max_i |1 - \tilde{\lambda}_{\pm}^{(i)}| \leq 1,$$

833 if and only if $h \leq 2\sqrt{s_d}/s_1$.

834 *Proof.* We directly compute

$$\begin{aligned} 835 \quad |1 - \tilde{\lambda}_{\pm}^{(i)}|^2 \leq 1 &\iff |1 - h\sqrt{s_d} \mp h\sqrt{s_d - s_i}|^2 \leq 1 \\ 836 \quad &\iff 1 - 2h\sqrt{s_d} + h^2s_i \leq 1 \\ 837 \quad &\iff h \leq 2\sqrt{s_d}/s_1. \quad \square \end{aligned}$$

838 THEOREM B.16. Consider the iteration given in Corollary 3.13. Suppose $a \geq$
 839 $\frac{2}{\sqrt{s_1 - \sqrt{s_d}}}$. We choose $\gamma = \gamma^* = as_d + 2\sqrt{s_d}$ and $0 < h \leq 1/(as_1 + \gamma^*)$. Then
 840 for $k \geq 1/h$ we have $\|Y_k\|_F \leq \tilde{C}h^2k^2(1 - \frac{h}{2}(as_d + \sqrt{s_d})^{2k-2})$, where the constant
 841 $\tilde{C} = d^2 \cdot \mathcal{O}(\text{poly}(\kappa))$.

Proof. Let us denote by $A = PJP^{-1}$ the Jordan decomposition of A . Then we know from (B.21) that A has precisely $2d - 1$ eigenvectors and one generalized eigenvector of algebraic multiplicity 2. Let $q_{\pm}^{(i)}, \dots, q_{\pm}^{(d-1)}$ be the eigenvectors with associated eigenvalues $\lambda_{\pm}^{(i)} = 1 - \tilde{\lambda}_{\pm}^{(i)}$, where $\tilde{\lambda}_{\pm}^{(i)}$ are from (B.21). With $\gamma = \gamma^*$, one has that $\tilde{\lambda}_+^{(d)} = \tilde{\lambda}_-^{(d)}$ is a generalized eigenvalue. Abusing notation, let us use $q_+^{(d)}$ to represent the eigenvector and $q_-^{(d)}$ to represent the generalized eigenvector of $\lambda_-^{(d)} = \lambda_+^{(d)}$. This means

$$Aq_+^{(d)} = \lambda_+^{(d)}q_+^{(d)}, \quad Aq_-^{(d)} = \lambda_-^{(d)}q_-^{(d)} + q_+^{(d)}.$$

We can express Y_0 by a basis representation

$$Y_0 = \sum_{\star, \diamond \in \{\pm\}} \sum_{i, j \leq d} \alpha_{\star, \diamond}^{i, j} q_{\star}^{(i)} (q_{\diamond}^{(j)})^T.$$

842 Then using Lemma B.11, we have that for $k \geq 1/h$,

$$\begin{aligned} 843 \quad \|Y_k\|_F &\leq 4d^2h^2k^2 \max_i |\lambda_{\pm}^{(i)}|^{2k-2} \max_{i, j, \star, \diamond} |\alpha_{\star, \diamond}^{i, j}| \|q_{\star}^{(i)} q_{\diamond}^{(j)}\|_F \\ 844 \quad (\text{B.23}) \quad &\leq 4d^2h^2k^2 \left(1 - \frac{h}{2}(as_d + \sqrt{s_d})\right)^{2k-2} \max_{i, j, \star, \diamond} |\alpha_{\star, \diamond}^{i, j}| \|q_{\star}^{(i)} q_{\diamond}^{(j)}\|_F. \end{aligned}$$

845 The second inequality is due to Lemma B.14. The maximum in the above is over
 846 $1 \leq i, j \leq d$ and $\star, \diamond \in \{\pm\}$. It remains to show that $\max_{i, j, \star, \diamond} |\alpha_{\star, \diamond}^{i, j}| \|q_{\star}^{(i)} q_{\diamond}^{(j)}\|_F =$
 847 $\mathcal{O}(\text{poly}(\kappa))$. Note that \mathbf{A} in Corollary 3.13 can be written as $\mathbf{A} = \mathbf{I} - h\tilde{\mathbf{G}}$ where $\tilde{\mathbf{G}}$
 848 does not depend on h when taking the first order approximation as in Lemma B.12.
 849 The rest of the argument is very similar to the proof of Lemma B.8 which we will not
 850 present due to brevity. We conclude that

$$\begin{aligned} 851 \quad \|Y_k\|_F &\leq d^2h^2k^2 \left(1 - \frac{h}{2}(as_d + \sqrt{s_d})\right)^{2k-2} \mathcal{O}(\text{poly}(\kappa)) \\ 852 \quad &= \tilde{C}h^2k^2 \left(1 - \frac{h}{2}(as_d + \sqrt{s_d})\right)^{2k-2}. \quad \square \end{aligned}$$

LEMMA B.17. A solution to the fixed point equation $\mathbf{Y}^* = \mathbf{A}\mathbf{Y}^*\mathbf{A}^T + \mathbf{L}\mathbf{L}^T$ where \mathbf{A} and \mathbf{L} are given in Proposition 3.11, is given by

$$\mathbf{Y}^* = \begin{pmatrix} Y_{11}^* & Y_{12}^* \\ Y_{12}^* & Y_{22}^* \end{pmatrix},$$

853 where $Y_{ij}^* \in \mathbb{R}^d$ are diagonal matrices. And the diagonal elements of Y_{ij}^* are given by

$$854 \quad (\text{B.24}) \quad Y_{11,i}^* = \frac{1}{s_i} \left(1 - \frac{hs_i(4 + (h + a(h\gamma - 2))(hs_i - \gamma + as_i(h\gamma - 1)))}{(hs_i - \gamma + as_i(h\gamma - 1))(4 + h(hs_i - 2\gamma + as_i(h\gamma - 2)))} \right),$$

$$855 \quad (\text{B.25}) \quad Y_{12,i}^* = \frac{2h(as_i - \gamma)}{(hs_i - \gamma + as_i(h\gamma - 1))(4 + h(hs_i - 2\gamma + as_i(h\gamma - 2)))},$$

$$856 \quad (\text{B.26}) \quad Y_{22,i}^* = \frac{-4\gamma - 2as_i(2 + h(hs_i - 3\gamma + as_i(h\gamma - 1)))}{(hs_i - \gamma + as_i(h\gamma - 1))(4 + h(hs_i - 2\gamma + as_i(h\gamma - 2)))}.$$

857 **Appendix C. Postponed proofs.**

858 *proof of Proposition 2.1.* We directly plug (2.19) into (2.18) and verify that we
859 recover (2.17).

$$\begin{aligned} 860 \quad & \nabla \cdot \left(\rho \operatorname{sym}(\mathbf{Q}) \nabla \log \frac{\rho}{\Pi} \right) + \nabla \cdot \left(\rho (\operatorname{sym}(\mathbf{Q}) \nabla \log(\Pi) + \mathbf{Q} \nabla H) \right) \\ 861 \quad & = \operatorname{sym}(\mathbf{Q}) : \nabla^2 \rho + \nabla \rho \operatorname{sym}(\mathbf{Q}) \nabla H + \rho \operatorname{sym}(\mathbf{Q}) : \nabla^2 H + \nabla \rho \operatorname{sym}(\mathbf{Q}) \nabla \log(\Pi) \\ 862 \quad & \quad + \rho \operatorname{sym}(\mathbf{Q}) : \nabla^2 \log(\Pi) + \nabla \cdot (\rho \mathbf{Q} \nabla H) \\ 863 \quad & = \operatorname{sym}(\mathbf{Q}) : \nabla^2 \rho + \nabla \cdot (\rho \mathbf{Q} \nabla H) \\ 864 \quad & = \nabla \cdot (\mathbf{Q} \nabla H \rho) + \sum_{i,j=1}^{2d} \frac{\partial^2}{\partial X_i \partial X_j} (Q_{ij} \rho), \end{aligned}$$

865 where we denote by $\mathbf{A} : \mathbf{B} = \sum_{i,j=1}^{2d} A_{ij} B_{ij}$ for $\mathbf{A}, \mathbf{B} \in \mathbb{R}^{d \times d}$. We have used
866 $\nabla \log(\Pi) = -\nabla H$ and $\nabla^2 \log(\Pi) = -\nabla^2 H$ to get the second equality. \square

867 *proof of Proposition 2.2.* We just need to verify that when $\rho(\mathbf{X}, t) = \Pi(\mathbf{X})$, we
868 have $\frac{\partial \rho}{\partial t} = 0$. It is clear that when $\rho(\mathbf{X}, t) = \Pi(\mathbf{X})$, the first term on the right hand
869 side of (2.18) is 0, since $\nabla \log(\frac{\rho}{\Pi}) = 0$. For the second term, let us use (2.19) to get

$$\begin{aligned} 870 \quad & \nabla \cdot (\Pi \Gamma) = \nabla \cdot (\Pi \mathbf{Q} \nabla H - \Pi \operatorname{sym}(\mathbf{Q}) \nabla \log(\Pi)) \\ 871 \quad & = \nabla \Pi \mathbf{Q} \nabla H + \Pi \mathbf{Q} : \nabla^2 H + \nabla \Pi \operatorname{sym}(\mathbf{Q}) \nabla \log(\Pi) + \Pi \operatorname{sym}(\mathbf{Q}) : \nabla^2 \log(\Pi) \\ 872 \quad & = -\Pi \nabla H \mathbf{Q} \nabla H + \Pi \mathbf{Q} : \nabla^2 H + \Pi \nabla H \operatorname{sym}(\mathbf{Q}) \nabla H + \Pi \operatorname{sym}(\mathbf{Q}) : \nabla^2 \log(\Pi) \\ 873 \quad & = \Pi \mathbf{Q} : \nabla^2 H + \Pi \operatorname{sym}(\mathbf{Q}) : \nabla^2 \log(\Pi) \\ 874 \quad & = \Pi \mathbf{Q} : \nabla^2 H - \Pi \operatorname{sym}(\mathbf{Q}) : \nabla^2 H \\ 875 \quad & = 0, \quad \square \end{aligned}$$

We have used $\nabla \Pi = -\Pi \nabla H$ to get the third equality. And we used $\nabla^2 \log(\Pi) = -\nabla^2 H$ to get the fifth equality. This proves that when $\rho = \Pi$, we indeed have

$$\frac{\partial \rho}{\partial t} \Big|_{\rho=\Pi} = \nabla \cdot \left(\Pi \operatorname{sym}(\mathbf{Q}) \nabla \log \frac{\Pi}{\Pi} \right) + \nabla \cdot (\Pi \Gamma) = 0 + 0 = 0.$$

proof of Proposition 3.2. With our choice of H , (2.15) is a multidimensional OU process. And since \mathbf{X}_0 follows a Gaussian distribution, it shows that \mathbf{X}_t will also be a Gaussian distribution. It is well known that the solution to (2.15) with H given by (3.3) is

$$\mathbf{X}_t = e^{-t\mathbf{Q}\tilde{\Sigma}^{-1}} \mathbf{X}_0 + \int_0^t e^{-(t-\tau)\mathbf{Q}\tilde{\Sigma}^{-1}} \sqrt{2 \operatorname{sym}(\mathbf{Q})} d\mathbf{B}_\tau.$$

The mean of \mathbf{X}_t is given by

$$\mathbb{E}\mathbf{X}_t = e^{-t\mathbf{Q}\tilde{\Sigma}^{-1}}\mathbb{E}\mathbf{X}_0 = 0.$$

876 We can compute the covariance $\Sigma(t)$ of \mathbf{X}_t . Since \mathbf{X}_t has zero mean, we obtain the
877 following using Ito's isometry

$$878 \quad (\text{C.1}) \quad \Sigma(t) = \mathbb{E}\mathbf{X}_t\mathbf{X}_t^T = 2 \int_0^t e^{-(t-\tau)\mathbf{Q}\tilde{\Sigma}^{-1}} \text{sym}(\mathbf{Q}) \left(e^{-(t-\tau)\mathbf{Q}\tilde{\Sigma}^{-1}} \right)^T d\tau + \mathbb{E}\mathbf{X}_0\mathbf{X}_0^T.$$

879 From the above expression, $\Sigma(t)$ is clearly well-defined, symmetric, positive definite
880 for all $t > 0$. We proceed by differentiating $\Sigma(t)$

$$\begin{aligned} 881 \quad \dot{\Sigma}(t) &= 2 \frac{d}{dt} \int_0^t e^{-(t-\tau)\mathbf{Q}\tilde{\Sigma}^{-1}} \text{sym}(\mathbf{Q}) \left(e^{-(t-\tau)\mathbf{Q}\tilde{\Sigma}^{-1}} \right)^T d\tau \\ 882 \quad &= 2 \text{sym}(\mathbf{Q}) + \int_0^t \frac{d}{dt} e^{-(t-\tau)\mathbf{Q}\tilde{\Sigma}^{-1}} \text{sym}(\mathbf{Q}) \left(e^{-(t-\tau)\mathbf{Q}\tilde{\Sigma}^{-1}} \right)^T d\tau \\ 883 \quad &= 2 \text{sym}(\mathbf{Q}) - \mathbf{Q}\tilde{\Sigma}^{-1}\Sigma(t) - \Sigma(t)\tilde{\Sigma}^{-1}\mathbf{Q}^T \\ 884 \quad &= 2 \text{sym}(\mathbf{Q}(\mathbf{I} - \tilde{\Sigma}^{-1}\Sigma)). \end{aligned}$$

885 This finishes the proof. □

886 **Acknowledgments.** X. Zuo is partially supported by AFOSR YIP award No.
887 FA9550-23-1-0087. X. Zuo and S. Osher are partially funded by STROBE NSF STC
888 DMR 1548924, AFOSR MURI FA9550-18-502 and ONR N00014-20-1-2787. W. Li
889 is partially supported by the AFOSR YIP award No. FA9550-23-1-0087, NSF DMS-
890 2245097, and NSF RTG: 2038080.

891 REFERENCES

- 892 [1] L. AMBROSIO, N. GIGLI, AND G. SAVARÉ, *Gradient flows: in metric spaces and in the space of*
893 *probability measures*, Springer Science & Business Media, 2008.
- 894 [2] C. ANDRIEU, N. DE FREITAS, A. DOUCET, AND M. I. JORDAN, *An introduction to MCMC for*
895 *machine learning*, Machine learning, 50 (2003), pp. 5–43.
- 896 [3] H. ATTOUCH, Z. CHBANI, J. FADILI, AND H. RIAHI, *First-order optimization algorithms via*
897 *inertial systems with Hessian driven damping*, Mathematical Programming, (2020), pp. 1–
898 43.
- 899 [4] H. ATTOUCH, Z. CHBANI, J. FADILI, AND H. RIAHI, *Convergence of iterates for first-order*
900 *optimization algorithms with inertia and Hessian driven damping*, Optimization, (2021),
901 pp. 1–40.
- 902 [5] H. ATTOUCH, Z. CHBANI, AND H. RIAHI, *Fast proximal methods via time scaling of damped*
903 *inertial dynamics*, SIAM Journal on Optimization, 29 (2019), pp. 2227–2256.
- 904 [6] C. H. BENNETT, *Mass tensor molecular dynamics*, Journal of Computational Physics, 19 (1975),
905 pp. 267–279.
- 906 [7] J. BESAG, *Comments on “Representations of knowledge in complex systems” by U. Grenander*
907 *and MI Miller*, J. Roy. Statist. Soc. Ser. B, 56 (1994), p. 4.
- 908 [8] Y. CAO, J. LU, AND L. WANG, *Complexity of randomized algorithms for underdamped Langevin*
909 *dynamics*, arXiv preprint arXiv:2003.09906, (2020).
- 910 [9] Y. CAO, J. LU, AND L. WANG, *On explicit L_2 -convergence rate estimate for underdamped*
911 *Langevin dynamics*, Archive for Rational Mechanics and Analysis, 247 (2023), p. 90.
- 912 [10] J. A. CARRILLO, Y.-P. CHOI, AND O. TSE, *Convergence to Equilibrium in Wasserstein Distance*
913 *for Damped Euler Equations with Interaction Forces*, Communications in Mathematical
914 Physics, 365 (2019), pp. 329–361.
- 915 [11] F. CASAS, J. M. SANZ-SERNA, AND L. SHAW, *Split hamiltonian monte carlo revisited*, Statistics
916 and Computing, 32 (2022), p. 86.

- 917 [12] A. CHAMBOLLE AND T. POCK, *A first-order primal-dual algorithm for convex problems with*
918 *applications to imaging*, Journal of mathematical imaging and vision, 40 (2011), pp. 120–
919 145.
- 920 [13] S. CHEN, Q. LI, O. TSE, AND S. J. WRIGHT, *Accelerating optimization over the space of*
921 *probability measures*, arXiv preprint arXiv:2310.04006, (2023).
- 922 [14] Y. CHEN, D. Z. HUANG, J. HUANG, S. REICH, AND A. M. STUART, *Gradient flows for sam-*
923 *pling: mean-field models, gaussian approximations and affine invariance*, arXiv preprint
924 arXiv:2302.11024, (2023).
- 925 [15] X. CHENG AND P. BARTLETT, *Convergence of Langevin MCMC in KL-divergence*, in Algorithmic
926 Learning Theory, PMLR, 2018, pp. 186–211.
- 927 [16] X. CHENG, N. S. CHATTERJI, P. L. BARTLETT, AND M. I. JORDAN, *Underdamped Langevin*
928 *MCMC: A non-asymptotic analysis*, in Conference on learning theory, PMLR, 2018,
929 pp. 300–323.
- 930 [17] S. CHEWI, P. R. GERBER, C. LU, T. LE GOUIC, AND P. RIGOLLET, *The query complexity*
931 *of sampling from strongly log-concave distributions in one dimension*, in Conference on
932 Learning Theory, PMLR, 2022, pp. 2041–2059.
- 933 [18] S. CHEWI, C. LU, K. AHN, X. CHENG, T. LE GOUIC, AND P. RIGOLLET, *Optimal dimension*
934 *dependence of the Metropolis-adjusted Langevin algorithm*, in Conference on Learning The-
935 ory, PMLR, 2021, pp. 1260–1300.
- 936 [19] A. DALALYAN, *Further and stronger analogy between sampling and optimization: Langevin*
937 *Monte Carlo and gradient descent*, in Conference on Learning Theory, PMLR, 2017,
938 pp. 678–689.
- 939 [20] A. S. DALALYAN, *Theoretical guarantees for approximate sampling from smooth and log-concave*
940 *densities*, Journal of the Royal Statistical Society Series B: Statistical Methodology, 79
941 (2017), pp. 651–676.
- 942 [21] A. S. DALALYAN AND A. KARAGULYAN, *User-friendly guarantees for the Langevin Monte Carlo*
943 *with inaccurate gradient*, Stochastic Processes and their Applications, 129 (2019), pp. 5278–
944 5311.
- 945 [22] A. S. DALALYAN AND L. RIOU-DURAND, *On sampling from a log-concave density using kinetic*
946 *Langevin diffusions*, Bernoulli, 26 (2020), pp. 1956–1988.
- 947 [23] M. DASHTI AND A. M. STUART, *The Bayesian approach to inverse problems*, arXiv preprint
948 arXiv:1302.6989, (2013).
- 949 [24] L. DEVROYE, A. MEHRABIAN, AND T. REDDAD, *The total variation distance between high-*
950 *dimensional Gaussians with the same mean*, arXiv preprint arXiv:1810.08693, (2018).
- 951 [25] A. DURMUS, S. MAJEWSKI, AND B. MIASOJEDOW, *Analysis of Langevin Monte Carlo via convex*
952 *optimization*, Journal of Machine Learning Research, 20 (2019), pp. 1–46.
- 953 [26] A. DURMUS AND E. MOULINES, *Nonasymptotic convergence analysis for the unadjusted*
954 *Langevin algorithm*, Annals of Applied Probability, 27 (2017), pp. 1551–1587.
- 955 [27] R. DWIVEDI, Y. CHEN, M. J. WAINWRIGHT, AND B. YU, *Log-concave sampling: Metropolis-*
956 *Hastings algorithms are fast*, Journal of Machine Learning Research, 20 (2019), pp. 1–42.
- 957 [28] Q. FENG, X. ZUO, AND W. LI, *Fisher information dissipation for time inhomogeneous stochas-*
958 *tic differential equations*, arXiv preprint arXiv:2402.01036, (2024).
- 959 [29] A. GARBUNO-INIGO, F. HOFFMANN, W. LI, AND A. M. STUART, *Interacting langevin diffusions:*
960 *Gradient structure and ensemble kalman sampler*, SIAM Journal on Applied Dynamical
961 Systems, 19 (2020), pp. 412–441.
- 962 [30] S. B. GELFAND AND S. K. MITTER, *Simulated annealing type algorithms for multivariate opti-*
963 *mization*, Algorithmica, 6 (1991), pp. 419–436.
- 964 [31] A. GELMAN, J. B. CARLIN, H. S. STERN, AND D. B. RUBIN, *Bayesian data analysis*, Chapman
965 and Hall/CRC, 1995.
- 966 [32] M. GIROLAMI AND B. CALDERHEAD, *Riemann manifold langevin and hamiltonian monte carlo*
967 *methods*, Journal of the Royal Statistical Society Series B: Statistical Methodology, 73
968 (2011), pp. 123–214.
- 969 [33] J. GOODMAN AND J. WEARE, *Ensemble samplers with affine invariance*, Communications in
970 applied mathematics and computational science, 5 (2010), pp. 65–80.
- 971 [34] Y. HE, K. BALASUBRAMANIAN, AND M. A. ERDOGDU, *On the ergodicity, bias and asymptotic*
972 *normality of randomized midpoint sampling method*, Advances in Neural Information Pro-
973 cessing Systems, 33 (2020), pp. 7366–7376.
- 974 [35] J. IDIER, *Bayesian approach to inverse problems*, John Wiley & Sons, 2013.
- 975 [36] P. IZMAILOV, S. VIKRAM, M. D. HOFFMAN, AND A. G. WILSON, *What are Bayesian neural*
976 *network posteriors really like?*, in International conference on machine learning, PMLR,
977 2021, pp. 4629–4640.
- 978 [37] R. JORDAN, D. KINDERLEHRER, AND F. OTTO, *The variational formulation of the Fokker–*

- 979 *Planck equation*, SIAM journal on mathematical analysis, 29 (1998), pp. 1–17.
- 980 [38] Y. T. LEE, R. SHEN, AND K. TIAN, *Logsmooth gradient concentration and tighter runtimes for*
 981 *Metropolized Hamiltonian Monte Carlo*, in Conference on learning theory, PMLR, 2020,
 982 pp. 2565–2597.
- 983 [39] B. LEIMKUHNER, C. MATTHEWS, AND J. WEARE, *Ensemble preconditioning for markov chain*
 984 *monte carlo simulation*, Statistics and Computing, 28 (2018), pp. 277–290.
- 985 [40] T. LELIEVRE, F. NIER, AND G. A. PAVLIOTIS, *Optimal non-reversible linear drift for the conver-*
 986 *gence to equilibrium of a diffusion*, Journal of Statistical Physics, 152 (2013), pp. 237–274.
- 987 [41] T. LELIÈVRE, G. A. PAVLIOTIS, G. ROBIN, R. SANTET, AND G. STOLTZ, *Optimizing the diffusion*
 988 *of overdamped langevin dynamics*, arXiv preprint arXiv:2404.12087, (2024).
- 989 [42] R. LI, H. ZHA, AND M. TAO, *Hessian-free high-resolution nesterov acceleration for sampling*,
 990 in International Conference on Machine Learning, PMLR, 2022, pp. 13125–13162.
- 991 [43] J. S. LIU, *Monte Carlo strategies in scientific computing*, vol. 10, Springer, 2001.
- 992 [44] Y.-A. MA, N. S. CHATTERJI, X. CHENG, N. FLAMMARION, P. L. BARTLETT, AND M. I. JORDAN,
 993 *Is there an analog of nesterov acceleration for gradient-based MCMC?*, Bernoulli, 27 (2021),
 994 pp. 1942–1992.
- 995 [45] D. J. MACKAY, *Bayesian neural networks and density networks*, Nuclear Instruments and
 996 Methods in Physics Research Section A: Accelerators, Spectrometers, Detectors and Asso-
 997 ciated Equipment, 354 (1995), pp. 73–80.
- 998 [46] D. J. MACKAY, *Information theory, inference and learning algorithms*, Cambridge university
 999 press, 2003.
- 1000 [47] C. J. MADDISON, D. PAULIN, Y. W. TEH, B. O'DONOGHUE, AND A. DOUCET, *Hamiltonian*
 1001 *descent methods*, arXiv preprint arXiv:1809.05042, (2018).
- 1002 [48] J. C. MATTINGLY, A. M. STUART, AND D. J. HIGHAM, *Ergodicity for SDEs and approxima-*
 1003 *tions: locally lipschitz vector fields and degenerate noise*, Stochastic processes and their
 1004 applications, 101 (2002), pp. 185–232.
- 1005 [49] S. P. MEYN AND R. L. TWEEDIE, *Markov chains and stochastic stability*, Springer Science &
 1006 Business Media, 2012.
- 1007 [50] W. MOU, Y.-A. MA, M. J. WAINWRIGHT, P. L. BARTLETT, AND M. I. JORDAN,
 1008 *High-order Langevin diffusion yields an accelerated MCMC algorithm*, arXiv preprint
 1009 arXiv:1908.10859, (2019).
- 1010 [51] R. M. NEAL, *Bayesian learning for neural networks*, vol. 118, Springer Science & Business
 1011 Media, 2012.
- 1012 [52] Y. E. NESTEROV, *A method of solving a convex programming problem with convergence rate*
 1013 $\mathcal{O}(\frac{1}{k^2})$, in Doklady Akademii Nauk, vol. 269, Russian Academy of Sciences, 1983, pp. 543–
 1014 547.
- 1015 [53] C. P. ROBERT, G. CASELLA, AND G. CASELLA, *Monte Carlo statistical methods*, vol. 2, Springer,
 1016 1999.
- 1017 [54] G. O. ROBERTS AND R. L. TWEEDIE, *Exponential convergence of Langevin distributions and*
 1018 *their discrete approximations*, Bernoulli, (1996), pp. 341–363.
- 1019 [55] R. SHEN AND Y. T. LEE, *The randomized midpoint method for log-concave sampling*, Advances
 1020 in Neural Information Processing Systems, 32 (2019).
- 1021 [56] A. M. STUART, *Inverse problems: a Bayesian perspective*, Acta numerica, 19 (2010), pp. 451–
 1022 559.
- 1023 [57] W. SU, S. BOYD, AND E. J. CANDÈS, *A differential equation for modeling Nesterov's accelerated*
 1024 *gradient method: Theory and insights*, Journal of Machine Learning Research, 17 (2016),
 1025 pp. 1–43.
- 1026 [58] A. TAGHVAEI AND P. MEHTA, *Accelerated flow for probability distributions*, in International
 1027 conference on machine learning, PMLR, 2019, pp. 6076–6085.
- 1028 [59] D. TALAY AND L. TUBARO, *Expansion of the global error for numerical schemes solving sto-*
 1029 *chastic differential equations*, Stochastic analysis and applications, 8 (1990), pp. 483–509.
- 1030 [60] H. Y. TAN, S. OSHER, AND W. LI, *Noise-free sampling algorithms via regularized Wasserstein*
 1031 *proximals*, arXiv preprint arXiv:2308.14945, (2023).
- 1032 [61] Y. W. TEH, A. THIÉRY, AND S. J. VOLLMER, *Consistency and fluctuations for stochastic*
 1033 *gradient Langevin dynamics*, Journal of Machine Learning Research, 17 (2016).
- 1034 [62] T. VALKONEN, *A primal–dual hybrid gradient method for nonlinear operators with applications*
 1035 *to mri*, Inverse Problems, 30 (2014), p. 055012.
- 1036 [63] S. VEMPALA AND A. WIBISONO, *Rapid convergence of the unadjusted Langevin algorithm:*
 1037 *Isoperimetry suffices*, Advances in neural information processing systems, 32 (2019).
- 1038 [64] Y. WANG AND W. LI, *Accelerated information gradient flow*, Journal of Scientific Computing,
 1039 90 (2022), pp. 1–47.
- 1040 [65] M. WELLING AND Y. W. TEH, *Bayesian learning via stochastic gradient Langevin dynamics*, in

- 1041 Proceedings of the 28th international conference on machine learning (ICML-11), Citeseer,
1042 2011, pp. 681–688.
- 1043 [66] S. ZHANG, S. CHEWI, M. LI, K. BALASUBRAMANIAN, AND M. A. ERDOGDU, *Improved dis-*
1044 *cretization analysis for underdamped Langevin Monte Carlo*, in The Thirty Sixth Annual
1045 Conference on Learning Theory, PMLR, 2023, pp. 36–71.
- 1046 [67] X. ZUO, S. OSHER, AND W. LI, *Primal-dual damping algorithms for optimization*, *Annals of*
1047 *Mathematical Sciences and Applications*, 9 (2024), pp. 467–504.